SAND2021-6364R

Dispenser Reliability: Materials R&D

A Hydrogen Fueling Infrastructure Research and Station Technology (H2FIRST) Report

Nalini C. Menon
Ethan S. Hecht
Sandia National Laboratories

Sandia National Laboratories is a multimission laboratory managed and operated by National Technology and Engineering Solutions of Sandia, LLC, a wholly owned subsidiary of Honeywell International Inc., for the U.S. Department of Energy's National Nuclear Security Administration under contract DE-NA0003525.

Technical Report
SAND2020-XXXX
December 2020

U.S. DEPARTMENT OF ENERGY | Energy Efficiency & Renewable Energy

NREL
NATIONAL RENEWABLE ENERGY LABORATORY

Sandia National Laboratories

Dispenser Reliability: Materials R&D

A Hydrogen Fueling Infrastructure Research and Station Technology (H2FIRST) Report

Nalini C. Menon, Ethan S. Hecht
Sandia National Laboratories

Sandia National Laboratories is a multimission laboratory managed and operated by National Technology and Engineering Solutions of Sandia, LLC, a wholly owned subsidiary of Honeywell International Inc., for the U.S. Department of Energy's National Nuclear Security Administration under contract DE-NA0003525.

Technical Report
SAND2020-xxxx
December 2020

Sandia National Laboratories
Albuquerque, New Mexico 87185
Livermore, California 94550
www.sandia.gov

Issued by Sandia National Laboratories, operated for the United States Department of Energy by National Technology & Engineering Solutions of Sandia, LLC.

Acknowledgments

This work is funded by the U.S. Department of Energy (DOE) Fuel Cell Technologies Office in the Office of Energy Efficiency and Renewable Energy.

The Hydrogen Fueling Infrastructure Research and Station Technology Project (H2FIRST) is a DOE project executed by Sandia National Laboratories and the National Renewable Energy Laboratory. The objective of H2FIRST is to ensure that fuel cell electric vehicle customers have a positive fueling experience relative to conventional gasoline/diesel stations as vehicles are introduced and transition to advanced refueling technology.

DOE's Fuel Cell Technologies Office established H2FIRST directly in support of H2USA, a public-private partnership co-launched by DOE and industry in 2013 to address the key challenges of hydrogen infrastructure.

In addition, the authors wish to thank the team, including April Nissen (SNL), Fitzjames Ryan (SNL), Chris Reed (SNL), Heidy Vega (SNL), Bernice Mills (SNL), Robert Oteri (SNL), Jeff Campbell (SNL), Mike Peters (NREL), Matt Ruple (NREL), Kevin Hartmann (NREL), and Erin Winkler (NREL) for their contributions to the project.

Nomenclature

Abbreviation	Definition
ALT	Accelerated life testing
ATR-FTIR	Attenuated total reflectance Fourier Transform infra-red spectroscopy
DUT	Devices under test
DMTA	Dynamic Mechanical Thermal Analysis
FCEV	Fuel cell electric vehicle
FKM	Fluoroelastomers
FTIR	Fourier Transform infra-red spectroscopy
H2FIRST	Hydrogen Fueling Infrastructure Research and Station Technology
HNBR	Hydrogenated Nitrile Butadiene Rubber
MFBF	Mean fills between failures
NBR	Nitrile Butadiene Rubber
NC Valves	Normally Closed Valves
NO Valves	Normally Open Valves
PEEK	Poly ether ether ketone
POM	Poly Oxy Methylene
PTFE	Poly Tetra Fluoro Ethylene
PUR	Polyurethane
TPU	Thermoplastic polyurethane

Executive Summary

Dispensers are the top cause of maintenance events and down-time at hydrogen fueling stations. In an effort to help characterize and enable improvements in dispenser reliability, an extensive accelerated lifetime testing set-up was designed and built at NREL involving components typically part of dispensing operations at fueling stations. Device Under Test (DUTs) included different components such as normally open valves, normally closed valves, fueling nozzles, breakaways devices and filters. Conditions of testing included pressures, and flow rates similar to light duty fuel cell electric vehicles fueling at -40°C, and -20°C for thousands of cycles in hydrogen. Tested components (failed and non-failed) were disassembled at SNL and polymeric O-rings were carefully retrieved and cataloged for chemical and physical characterization. Data collected was compared to similar O-rings from unexposed or non-tested components for hydrogen effects, and failure modes. Degradation analyses, based on select polymer chemistries common across all component types, their location within components, visual assessment of damage coupled with strong hydrogen effects from chemical characterization, was completed and presented to NREL and DOE. Overall, the failure rate amongst the components was not as high as expected for the test conditions. Among the component types tested, breakaways were the most susceptible to damage under these test conditions, with fueling nozzles a close second. The proper combination of selection of the right polymer and optimum component design was found to make a strong difference in component reliability under severe dispenser operating conditions. Physical degradation of polymers, rather than chemical changes due to low temperature hydrogen exposure, is more prevalent as failure mode for these test conditions. The nature and the extent of the degradation was much less at -20°C as compared to -40°C. The damage and failure rates were higher at lower temperatures than at higher test temperatures. As expected, increasing the number of cycles at the lowest test temperature (-40°C) increased damage. This indicates that cycling at the low temperature of -40°C required by SAE J2601 can reduce component life in fuel dispensing operations.

Table of Contents

List of Figures

List of Tables

1 Background

The Hydrogen Fueling Infrastructure Research and Station Technology H2FIRST is a project launched by the US DOE's Hydrogen and Fuel Cells Technologies Office (HFTO) within the Office of Energy Efficiency and Renewable Energy (EERE), leveraging capabilities at the national laboratories to address the technology challenges related to hydrogen refueling stations. Led by Sandia National Laboratories (SNL) and National Renewable Energy Laboratory (NREL) and propelled by a broad array of public and private partners, H2FIRST is a strong example of the DOE's efforts to bring national lab capabilities and facilities to bear on both immediate and mid-term challenges faced by industry.

H2FIRST was established by the DOE's HFTO directly in support of H2USA, a public-private partnership co-launched by the DOE and industry in 2013. Its mission is to ensure that fuel cell electric vehicle (FCEV) customers have a positive fueling experience similar to conventional gasoline/diesel stations as these vehicles and transition to advanced fueling technology is aided. H2FIRST continues to help enable commercially viable hydrogen fueling stations by coordinating and leveraging the vast technical resources of its public and private sector participants. The H2FIRST activities positively impact the cost, reliability, safety, and consumer experience of FCEV stations and the project's technical work fills the most critical gaps and needs for achieving better performing and less expensive hydrogen fueling infrastructure. The development and application of physical testing, numerical simulation, and technology validation help identify and create low-cost, high-performance materials, components, systems, and station architectures.

A number of projects have been placed under the auspices of the H2FIRST initiative over the years. The purpose of this report is to provide details on dispenser reliability work in the timeframe FY 2016-2020. The main goal of this effort was to improve reliability and enable the prediction of the lifetime of fueling and dispensing components exposed to pre-cooled hydrogen at high pressures. The approach was to perform component testing under realistic conditions and perform material analyses to follow the progression of degradation.

In a retail hydrogen fueling station, the dispenser is typically connected to a high-pressure hydrogen source that enables the required pressure ramp rate, which is controlled via a variable area control device within the dispenser. The SAE J2601 fueling protocol determines the rate at which a dispenser should fill a vehicle (i.e., "ramp rate") to ensure a safe, fast fill [1]. The fueling pressure ramp rate at the dispenser depends on the hydrogen precooling temperature at the dispenser, the vehicle tank's volume and initial pressure, and the ambient temperature. At a fueling station, hydrogen in bulk storage is approximately at ambient temperature. However, fast dispensing increases the temperature of both the hydrogen and the vehicle tank liner, such that the hydrogen must be cooled to -40°C before it is dispensed to keep the FCEV tank from exceeding its maximum operating temperature of 85℃ and to prevent degradation of the tank liner.

The hydrogen fuel delivery temperature at the dispenser breakaway cannot be less than -40℃ or greater than -17.5°C at any time during the fueling process. The temperature of the hydrogen being dispensed (i.e., pre-cooling temperature) is an important parameter to ensure safety of the fueling process, so it is monitored throughout the fill. The station should achieve the precooling temperature consistent with the station type within the first 30 seconds of fueling. Dispensers are the top cause of maintenance events and down-time at hydrogen fueling stations (Figure 1), likely due to the low operating temperature of components. A lack of hydrogen refueling infrastructure performance data from earlier campaigns on performance of piping components at fueling dispenser conditions which provided only qualitative information, was a driver for this study [2].

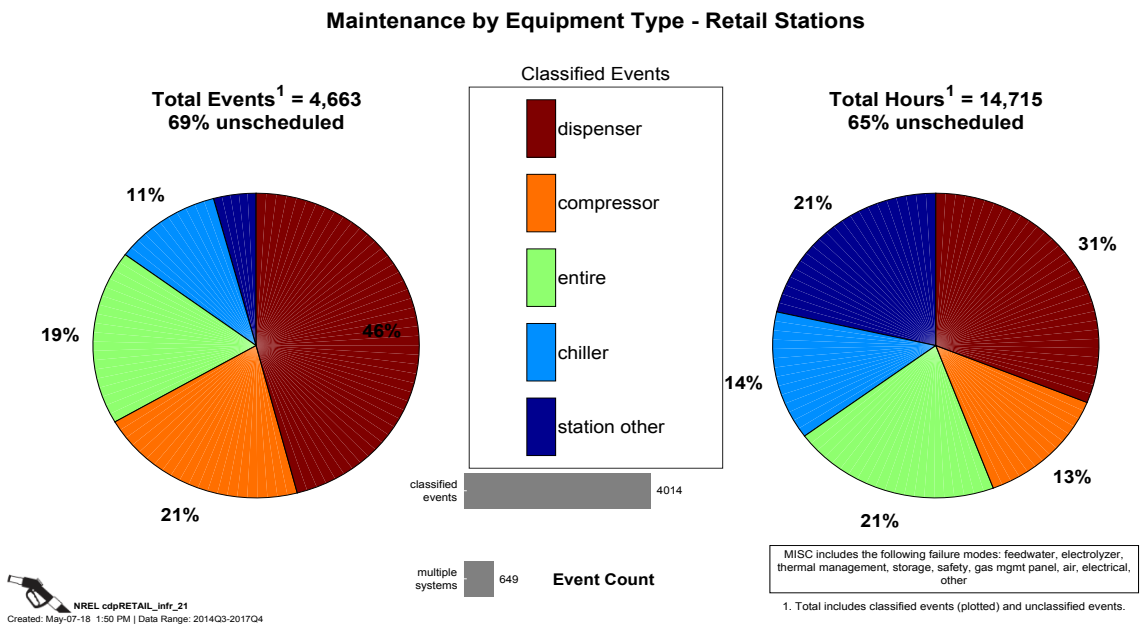

Figure 1. Dispensers are the top cause of maintenance events and downtime at hydrogen stations

1.1 Light Duty Dispenser Reliability study

A data review by Harty et al. (2010) [3] examined both temperature and pressure effects to suggest the optimal refueling method for FCEVs. This paper describes component testing results which indicate a need for substantial increase in reliability for the current -40°C pre-cooling specification under SAE J2601. It was clear that component design and materials selection could be improved. Pursuant to this, the Light Duty Dispenser Reliability project was launched in late 2015.

Accelerated Life Testing (ALT) was used to study reliability by placing commonly used hydrogen components in the pre-chilled portion of the dispenser under test in a laboratory environment. The goal of the ALT was to show the reliability differences of different hydrogen components, all part of the dispensing operation, while operating under extremely low temperatures (-40°C and -20°C), and to measure the advantage of increasing the pre-chilled hydrogen temperature requirement (to -20°C). The focus of the testing was on components commonly found in hydrogen dispensers. Component manufacturer support was solicited for this study with positive outcomes. For each type of component, more than one manufacturer was engaged for purchase of the parts.

The NREL team-led tasks focused on acquiring components from the manufacturers, developing a flow system and conducting ALT. The recirculation dispenser that they developed provides the same flow rate and pressure profiles as components in the chilled section of a real-world dispenser, including variation in the hydrogen gas temperature. More details on test conditions will be described in the next section. This work was completed at NREL's Hydrogen Infrastructure Testing and Research Facility (HITRF). Reliability at different temperatures was compared using root cause analysis of failures and Weibull estimates for reliability. A separate report with the findings of this task will be published by the NREL team.

Sandia's tasks as a part of the dispenser reliability study focused on material characterization of polymers removed from new, failed, and used (but working) components from the ALT. It is important to understand failure modes and degradation mechanisms of soft materials under test conditions to predict lifetimes and therefore dispenser reliability. A preliminary step to completing the material characterization was the disassembly of the components removed from testing at NREL

and careful removal of the polymeric O-rings without inducing handling damage. For all components tested, there was no information available on O-ring pedigree, and therefore identification of O-ring composition and establishment of baseline properties for unexposed O-rings was necessary. The same characterization methods were performed on all elastomeric and thermoplastic O-rings removed from tested components to determine the impact of hydrogen exposure at low temperature on polymer behavior. Chemical and physical properties including the glass transition temperature, storage modulus, mass, and density were evaluated for differences between exposed and non-exposed components. For elastomers, an additional property such as compression set ,confirmed the effects of varying hydrogen temperatures on these materials.

Degradation analyses of polymers was completed by either focusing on the failure of a specific component from different suppliers or on a common polymer across a maximum number of components. The latter approach was eventually implemented as it was more practical to follow the failure modes and mechanisms for one or two select chemistries common to components and easy to distinguish between contributions from component design vs material choice in these components. All analyses results were shared with NREL and combined with their survival analyses and modeling efforts to determine final conclusions and direct future efforts.

1.2 NREL Accelerated Lifetime Test Conditions

NREL's Accelerated Reliability Testing measures the mean fills between failures (MFBF) and mean kilograms between failures (MKBF) of hydrogen components subjected to pressures, ramp rates and flow rates similar to light duty fuel cell electric vehicle fueling at -40°C and -20°C. The reasoning behind NREL's tests was based on NFCTEC (National Fuel Cell Technology Evaluation Center) data and interviews with station operators that highlighted that components in the chilled section of the dispenser were the most likely to fail. Initially, following SAEJ2601 protocol, -40°C was selected as one of the test temperatures with additional temperatures of -20°C, 0°C and ambient temperature [4]. However, fueling practicality and budget restrictions limited the scope to two temperatures: -40°C and -20°C. The number of test cycles were limited to a little over 1000 cycles at each temperature for similar reasons. It was also certain that these 1000-cycle exposures, when successful, would provide initial evidence of the influence of cycling and temperatures on the polymers and could guide the optimization of future test conditions. Flow rates and pressure profiles were kept constant for both temperatures. Test factors and response variables are summarized in Table 1 below.

Table 1. Fixed factors, variable factors and response variables in Accelerated Lifetime Testing

Fixed Factors	Variable Factors			
Controlled	**Controlled**		**Uncontrolled**	
H_2 pressure ramp rate (> 17.6 MPa/min)	H_2 temperature	-40°C, -20°C	Ambient temperature	10°C - 40°C
H_2 flow rate (0.8 kg/min)	Component types	Nozzles Breakaways NO valves NC valves Filters	Ambient humidity	0 - 100%
H_2 pressure range (14.7-77.9 MPa)				

Response Variables	
H_2 leak (qualitative)	Yes or No
Fills before failure (quantitative)	Number
Amount of H_2 through component before failure (quantitative)	Kilograms

Components tested include normally open valves, normally closed valves, filters, dispensing nozzles, and breakaways. Normally open valves are designed to release flow through the valve and are commonly used for emergency safety. During normal operation, these are closed and when the system experiences failure (e.g., overpressure), the valve opens and allows the pressure to normalize. Normally closed valves typically allow gas or liquid to flow through the system and under abnormal conditions (e.g., loss of power) will close to isolate different sections of the flow system. Filters are used to remove particulates and other contaminants from the gas stream and ensure optimum purity of the compressed hydrogen dispensed. Dispensing nozzles are used to couple the dispenser to the vehicle, allowing a high flow rate and short filling times. These are designed to handle pressures of 70 MPa (10,000 psi) and 35 MPa (5000 psi) [4]. Breakaways are used to protect the dispenser in case of accidental "drive-off" while the nozzle is connected to the vehicle and permit safe separation of the nozzle from the dispenser, thus preventing damage to the dispenser.

Multiple units of the same type of component were procured from at least two different manufacturers per component type. Twenty-five units of each component per manufacturer were tested at each temperature in test loops designed for the purpose. A typical set-up is shown in Figure 2 and a schematic of multiple test set-ups is shown in Figure 3. Photographs of the multi-test set-up and the devices under test at NREL are shown in Figure 4.

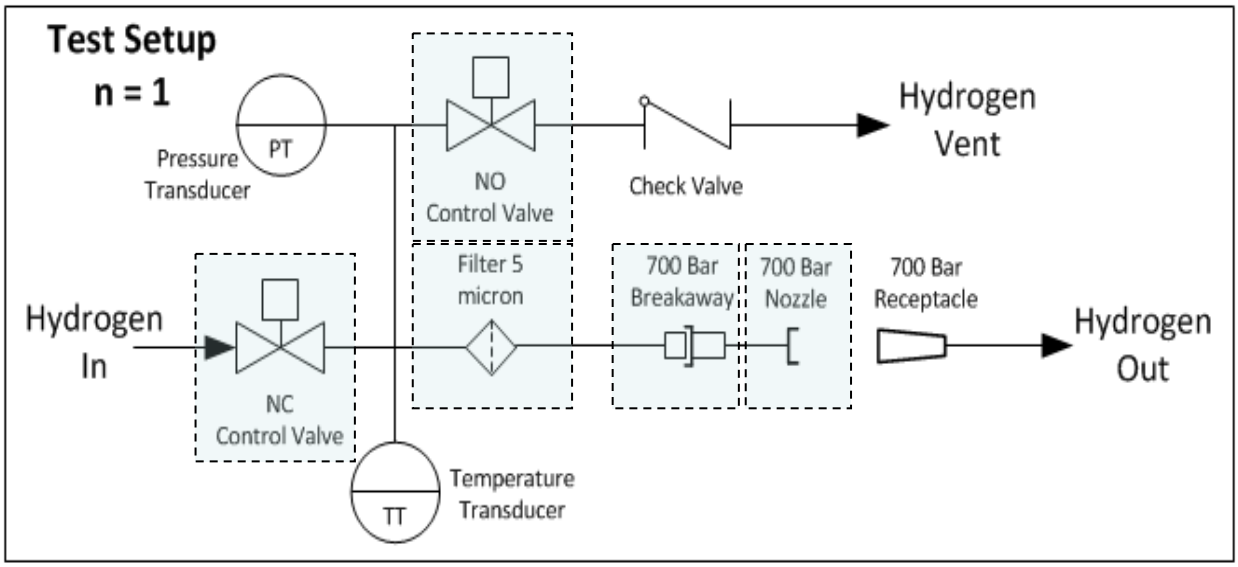

Figure 2. Schematic of different components (shown in highlighted boxes) in a test loop part of the Accelerated Lifetime Test

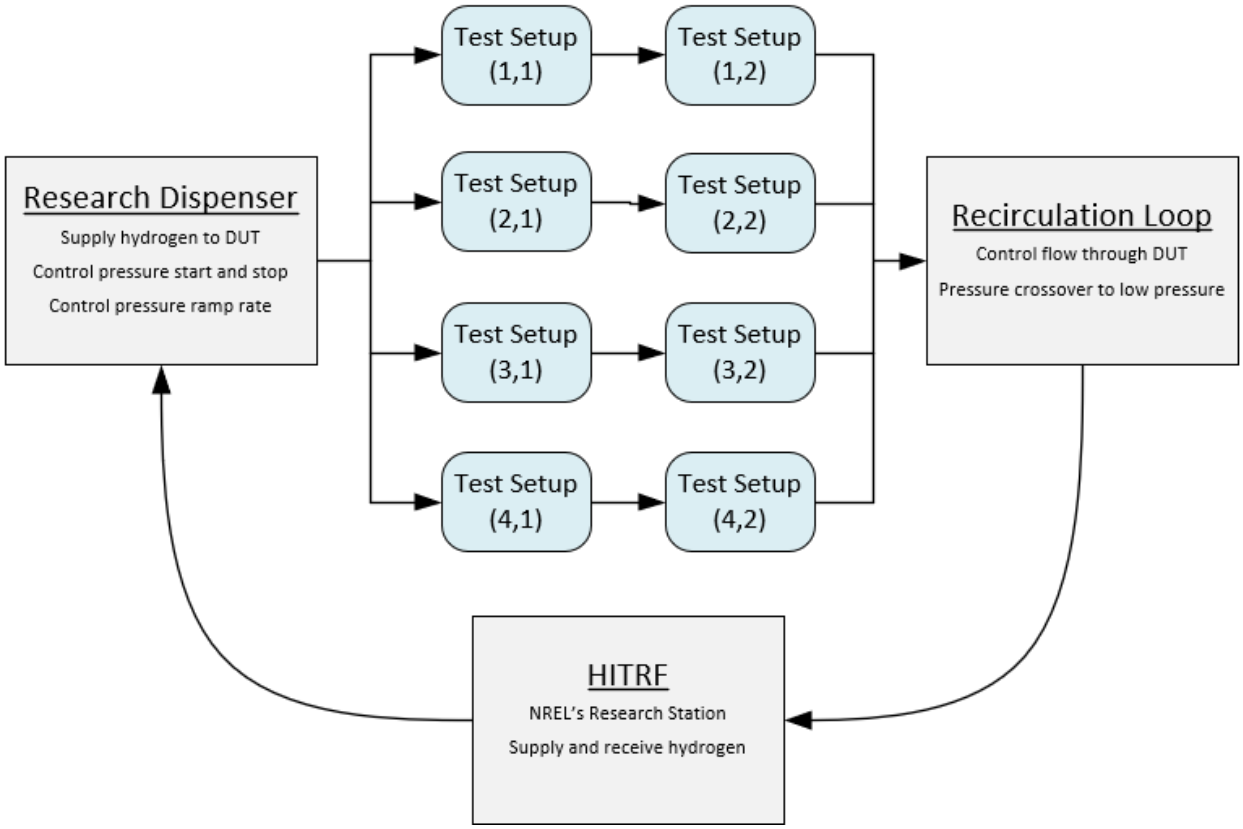

Figure 3. Schematic of recirculation loop with multiple test set-ups in the Accelerated Lifetime Test

Figure 4. Photographs of the multi-test set-up with the devices under test (DUT) at NREL

For each set of test cycles, failed components were removed upon failure from the loop while those that remained functional were part of it until completion of the test. A total of 71 components were shipped to Sandia with 12 unexposed components for baseline testing, 33 components from -40°C testing and 26 components from -20°C testing.

2 SNL Materials R&D

2.1 Component Disassembly

Sandia National Labs was responsible for materials R&D in relation to the components tested as part of NREL's Accelerated Lifetime Tests. Whole components including unexposed, failed and non-failed components marked with NREL designations were shipped to Sandia in five different shipments. Not all components tested were shipped to Sandia to keep material analyses within practical limits. These were catalogued in a database upon receipt. Figure 5 shows the total number of components received per component type for each test temperature, as a portion of the total components tested by NREL. All components received were disassembled. However, it should be noted from the figure that given the significantly large number polymeric materials per component, not all components received were analyzed. A total of 71 components were received with 12 unexposed components, 33 components tested at -40°C, and 26 components tested at -20°C. Except for the ones that failed earlier, all components were exposed to slightly over 1000 cycles at each temperature. Of these 71 components received at SNL, 22 contained no polymeric materials: these included filters (10), receptacles (10), mixing valves (1), and flowmeters (1). These 22 components were therefore not analyzed at SNL. The other component types are summarized in Figure 5.

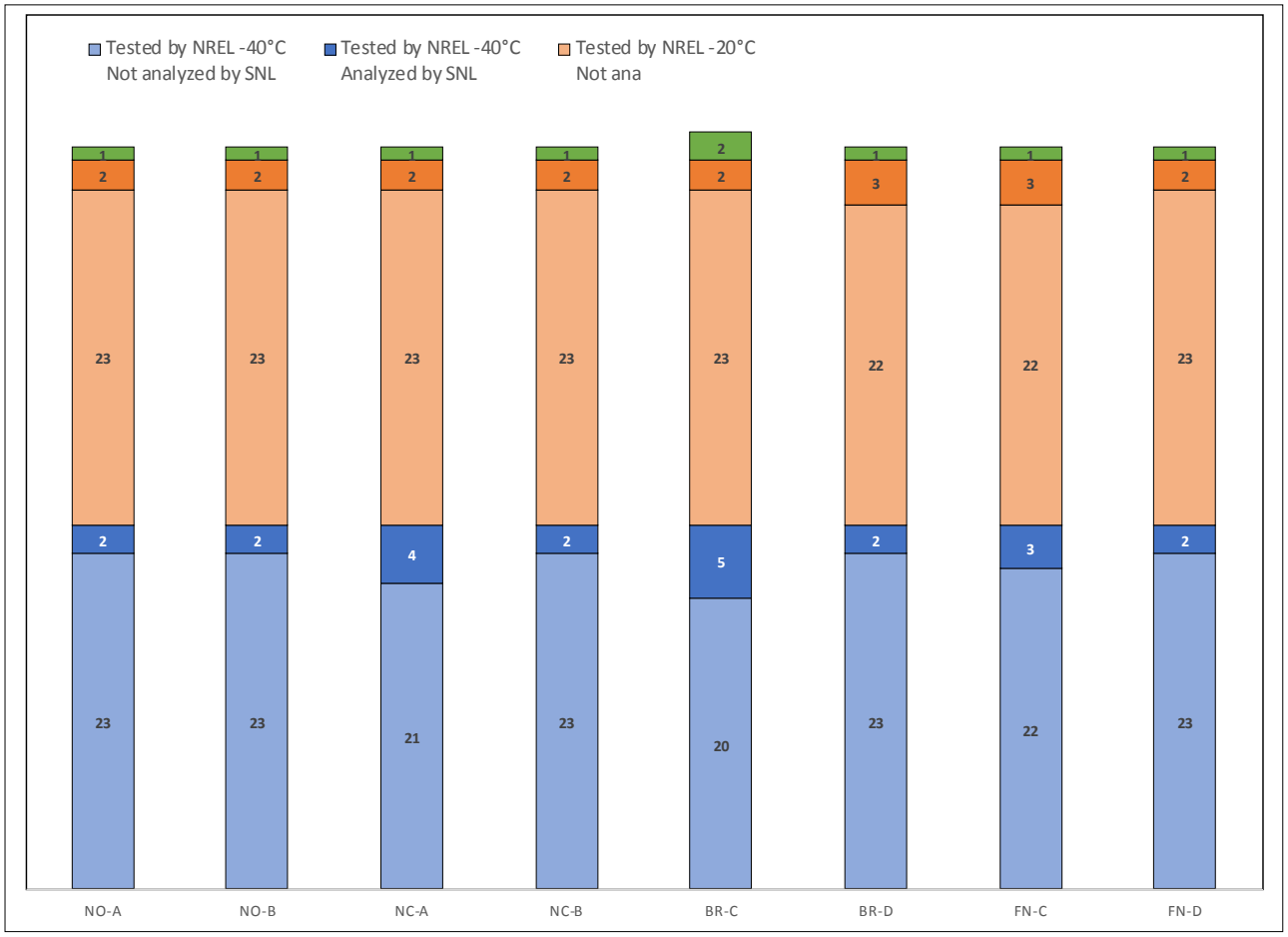

Figure 5. NREL ALT tested and SNL analyzed components: NO = Normally open; NC = Normally closed: BR = Breakaway; FN = Fueling nozzles; A, B, C, D stand for protected manufacturer IDs

The disassembly of these components was quite unfamiliar and therefore time-consuming for the Sandia team. We relied heavily on manufacturer-supplied drawings for components from one manufacturer for this activity. All of the remaining components were disassembled purely based on consultation with Sandia SMEs. Images of whole components were captured before disassembly and also for each step in the disassembly process. The order of removal of sub-components and the number of O-rings removed was carefully recorded during the disassembly of unexposed components so that the same procedures could be followed with the exposed ones. Disassembly was especially important with respect to being able to collect O-rings from each component respective to location for characterization before and after hydrogen exposure.

Components were disassembled carefully with special tools so as to not alter the physical form of each polymer part. O-rings were retrieved and bagged individually with careful assignment of SNL identifiers to each component, comprised of a combination of component source and location within the component. The number of O-rings removed differed from component to component but matched for unexposed, failed, and non-failed components of the same type for the same manufacturer. Also, O ring chemistry varied from elastomeric to thermoplastic in nature. After removal from the components, the O-rings were prepared for characterization tests towards identification of polymer chemistries and chemical and physical properties.

Characterization methods for the polymers were established at first with non-exposed O-rings. These methods were then used for analyses of exposed O-rings such that direct comparisons were possible.

Thermoplastics and elastomers received analyses that were common to both types of polymers. There were also analyses that were specific to each material type. More details on the characterization are described in Section 3.

3 Materials Characterization

3.1 Overcoming Challenges in material analyses

Polymer physical and chemical property changes are important to recognize for their impact on the functioning of H_2 dispensing equipment. For example, compression set property changes in sealing elastomers within the dispensing components at low temperatures can lead to leaks as the temperature rises. Under extreme conditions, these elastomers can exhibit cold brittle catastrophic failure. The combined repeated assault of high pressures, cold temperatures, and cycling on polymers can cause failure which in turn leads to station down-time and related costs.

The main focus of materials characterization was to evaluate the changes in polymer physical and chemical properties via typical characterization methods on polymeric O-rings from actual tested components, in order to establish failure modes and predict component lifetimes towards assessing dispenser reliability. Baseline properties were first established with unexposed components. All exposed components received were disassembled and the O-rings were removed for chemical analyses. For the components received and disassembled, over 350 specimens were analyzed to establish polymer chemistries and their vulnerability towards cold H_2 cycling conditions and identify their failure modes so as to inform degradation analyses.

There were two challenges encountered with materials characterization work that are worth mentioning. The first has to do with the reality that component manufacturers select polymers in their components based on their materials research and suitability to their design. This is proprietary information, not openly published or shared. The proprietary nature of polymeric materials per component type required that we identify the chemistry of the polymers obtained from the disassembly without prior knowledge of the same. There was only one NDA (non-disclosure agreement) in place with one of the manufacturers that helped us verify our chemical identification of the polymers against manufacture-provided data on actual O-ring chemistries within their component. Polymeric material identification for all other components was based on the material characterization analyses (often complementary to each other) which helped establish the unknown chemistries of the polymers accurately.

The second challenge we recognized was that polymer degradation due to hydrogen can happen only to those O-rings that are actually exposed to hydrogen. Each component has a number of O-rings that are not in H_2-exposed locations within the component and hence, are not relevant to the degradation analyses. This information is again proprietary to the manufacturer and was not available to us. Therefore, initially, we compared all polymers from all the unexposed components to the failed or non-failed polymers from the same components. The more susceptible chemistries could be quickly identified from the first set of failed and exposed component and at that point, it made sense to limit our characterization and failure mode analyses to those particular ones.

3.2 Characterization methods

The characterization methods were selected as a subset of standard analyses for polymers, based on the sensitivity of the method to measure the expected property changes, constrained by the specimen sizes and shapes that could be prepared from the various O-rings. Figure 6 shows the methods selected for analyses of thermoplastics and elastomers.

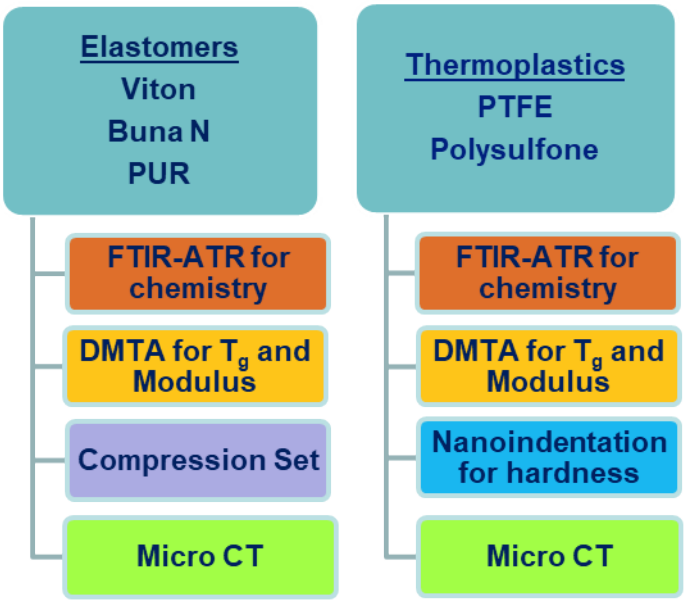

Figure 6. Characterization methods selected for analyses of O-rings from components

For both elastomers and thermoplastic samples, Attenuated Total Reflectance-Fourier Transform Infra-red Spectroscopy (ATR-FTIR) was used to examine surface chemistry and changes thereof. This is a non-destructive method and preceded all destructive types of analyses. Dynamic Mechanical Thermal Analysis (DMTA) is a thermal characterization method that can measure mechanical transformations such as change in storage modulus and glass transition temperatures for polymers. Compression set measurement is specific to elastomers because they are compressible and can see permanent deformation in service; nanoindentation is the best method to measure hardness and modulus (stiffness) changes in thermoplastics. DMTA and compression set measurements are destructive test methods and were only performed on specimens after they were previously evaluated by the non-destructive methods. Micro computed tomography (Micro-CT) is a useful tool to examine the specimens for internal voids and cracks after hydrogen exposure. Optical microscopy using a Keyence microscope was used to evaluate surface texturization effects, blisters, external cracks and damage in the form of bubbles, tears and shredding in the specimens. All details of the test methods are described in detail in the following sections.

A significant takeaway from the materials characterization was that a multi-technique effort was necessary for both identification of the polymers and the detection of hydrogen effects. For example, the collection of ATR-FTIR spectra for elastomers was challenging because of the difficulty in maintaining proper contact with the resilient sample surface. This resulted in spectra with significant background noise and low peak intensities, making separation and identification of important peaks difficult. However, when ATR-FTIR identification was supplemented with glass transition and modulus data for the same polymer from DMTA, it was easy to confirm the chemical identity of the polymer and match it to standard data in the NIST Chemistry Web Book SRD 69 database. All analyses were performed this way, with confirmation of both polymer chemistry and hydrogen effects based on multiple characterization methods, so as to achieve more reliable data and greater confidence in the determinations and conclusions from the study.

3.2.1 Attenuated Total Reflectance-Fourier Transform Infra-Red Spectroscopy (ATR-FTIR)

Fourier transform Infra-Red Spectroscopy (FTIR) is used to analyze the molecular structure of materials, based on the absorption of wavelengths from an incident IR beam on a sample. The method is non-destructive but surface-focused (0.5-5 μm depth). In this project, an Attenuated Total Reflectance sampling technique was used wherein a germanium crystal focuses the incident beam onto the sample, allowing the absorption of specific wavelengths and transmitting the remaining wavelengths back through the crystal to the detector. The incident light energy absorbed by the molecules cause them to undergo bending, rotational, and vibrational modes of molecular motion, which is unique to the functional groups present on the molecule. The absorption intensity is plotted against the wavenumber (cm^{-1}) to provide a spectrum. Most polymers have a "fingerprint" over a wavenumber range of 1500 to 500 cm^{-1} where each polymer has a unique molecular structure that can be identified. For our project, ATR-FTIR spectra was collected on all materials to allow a comparison of the unexposed to the exposed spectra for the individual material types which would indicate a chemical change due to exposure to H_2 under the test conditions. Observed changes to the FTIR spectra due to H_2 exposure are permanent.

3.2.2 Dynamic Mechanical Thermal Analysis (DMTA)

Dynamic Mechanical Thermal Analysis is used to characterize polymers for their viscoelastic properties. In this method, a sinusoidal strain is applied to the sample, and the resulting stress response is separated into two portions. The storage modulus (G') is the elastic portion of the response, which is in phase with the oscillating strain, and the loss modulus (G") is the viscous portion of the response, out of phase with the strain. These moduli, and the glass transition temperature (T_g) indicated by peaks and step changes in their curves as a function of temperature, are some of the polymer properties that can be characterized using this method. This analysis method can be used with both thermoplastics and elastomers but is a destructive analysis method. For our project, DMTA using a TA instruments DHR-2 Hybrid Rheometer was used to examine the viscoelastic properties of the polymers. Measurements were typically made in duplicate. Specimens were examined using the Rectangular Torsion geometry under strains ranging from 0.1% to 1% depending on material and sample form factor. Also a frequency of 1 Hz, with heating at a rate of 5°C/minute over the temperature range -100°C to 200°C was used, except for high glass transition temperature plastic PTFE for which a temperature range of 0°C to 250°C was used A change in either moduli or T_g after H_2 exposure for materials in our study was indicative of permanent changes within the polymer due to testing.

3.2.3 Compression Set

Compression set provides information on the permanent deformation in elastomeric polymers during the application of a compressive force at a given temperature, % compression, and duration of compression. This permanent deformation can lead to a decrease in sealing force provided by the polymer, and ultimately leakage. When elastomers are exposed to hydrogen, free volume changes and weak interactions with hydrogen can either temporarily or permanently influence their compression set properties. Figure 7 shows the compression test set-up used for elastomers. Due to the limited number of specimens, typically only single measurements of each part were completed. After the starting thickness of each specimen is measured with a laser micrometer, the specimens were placed on the bottom plate of the compression set-up. A constant deflection to 75% of the starting thickness (25% compression), created by clamping down the top plate of the set-up and controlled by a steel spacer bar placed alongside the specimen, is exerted on the samples at a temperature of 110°C over a period of 22 hours (ASTM D 395 Method B). After removal from the

compression set-up, the specimen is allowed to recover for 30 minutes at room temperature. The final thickness of the specimen is measured again with the laser micrometer. Compression set is expressed as a percentage of the original deflection:

$C_B = [(t_o - t_1)/ (t_o - t_n)] \text{ X } 100$

where

C_B = Compression set (%)

t_o = original thickness of the specimen

t_1 = final thickness of the specimen

t_n = thickness of the spacer bar

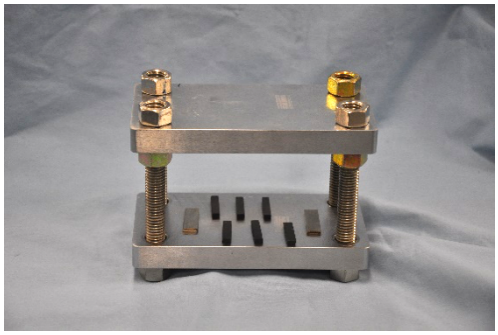

Figure 7. Compression set test set-up for elastomers. The black polymer specimens (center) are compressed to the thickness of the steel spacer bars on either side by lowering the top plate (currently raised for demonstration purposes)

3.2.4 Nanoindentation

Nanoindentation is used to measure hardness, elastic modulus, and the coefficient of friction of rigid polymers. A 2-µm conical tip is used to either press against the surface to measure hardness and elastic modulus or to generate wear cycles on the surface of the sample. By applying a small oscillating force to the tip, the hardness and elastic modulus of the sample as a function of depth is measured. Wear cycles were performed in groups of 10 cycles (back and forth) covering a 5-µm length at a constant load of 25 µN. Five of these 10 cycles were grouped, and friction was calculated for each forward segment of a cycle. Surface texturization effects and their contribution were evaluated afterwards. This method is non-destructive and measures permanent changes in hardness of the material.

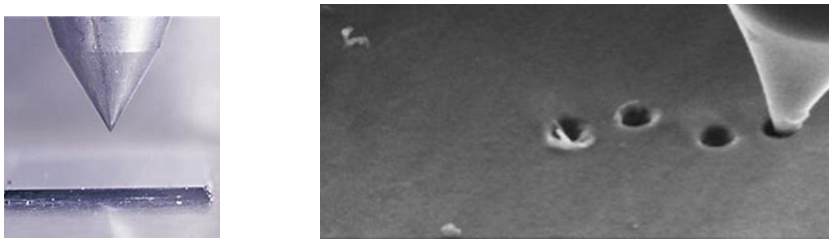

Figure 8. Nanoindentation conical tip being used to test hardness and elastic modulus of a surface

3.2.5 Micro Computer Tomography (Micro CT)

Internal microstructural damage in the elastomers was characterized by optical microscopy and micro computed tomography (Micro-CT). Microstructural damage was not explored in the thermoplastics

because, unlike the elastomers, there was no evidence of damage upon surface examination. Micro-CT is a high-resolution 3D microscopy technique that non-destructively images the fine scale internal structure (especially voids) in polymers. Mounted samples of polymer O-rings are rotated in the presence of X-rays as a detector collects images that are used to create a 3-D rendering of surfaces with spatial resolution in the micrometer range. Micro-CT images enable the identification of structural defects (such as voids and cracks) in the polymers due to gas exposure.

4 Results and discussion

Survival analyses were conducted by NREL for each test and materials characterization performed on components as they were received at SNL, in batches. As the rate of failure of the components under the stringent test conditions was slower and smaller in numbers than expected, it was decided to forego 0°C testing and limit the testing to -40°C and -20°C H_2 exposure. At least 25 of each component type and a total of nine different components were exposed to hydrogen at characteristic vehicle fueling pressure ramps up to 70 MPa (700 bar or 10,000 psi) at these temperatures. Polymers were harvested and studied from normally open valves, normally closed valves, breakaways, and fueling nozzles. Although filters were included in the low temperature testing, there were no polymers found in this component and hence, no further filters were disassembled or analyzed. O-rings removed from exposed components were compared with those from the same type of unexposed component. Based on the multi-technique materials characterization approach, the common polymers identified in the various components are shown in Table 2 below. Each component type was procured from at least two manufacturers to allow for inclusion of different designs, manufacturing effects and possibly different choices of polymers. All manufacturer IDs have been protected.

Table 2. Common polymers identified in components analyzed based on materials characterization (here A, B, C and D are manufacturers with protected IDs)

Component Type	NO Valves		NC Valves		Breakaways		Fueling Nozzles	
Component	NO-A	NO-B	NC-A	NC-B	BR-C	BR-D	FN-C	FN-D
Components analyzed/tested	4/50	4/50	6/50	4/50	7/50	5/50	6/50	4/50
PTFE								
NBR								
PEEK								

It is clear from Table 2 that PTFE (Polytetrafluorethylene) is the most common polymer, found in 29 of the 40 components both tested and analyzed. Superior performance properties of this polymer such as the low coefficient of friction, high flexural strength (even at low temperatures), dimensional stability, and inertness to chemical attack are well-known and likely the reasons for the selection. In addition to PTFE, the use of Buna N or NBR (nitrile butadiene rubber) and PEEK (polyetheretherketone) are also somewhat common. Along with these common polymers, polymers found in these components included polyurethane, butyl rubber, neoprene, POM (polyoxymethylene) and HNBR (hydrogenated nitrile butadiene rubber). In this study, we chose to focus on the polymers that were the most common to all the components, regardless of type or manufacturer. This way, degradation analyses can separate effects of fixturing from polymer chemistry, providing more

insight into polymer compatibility behavior in hydrogen under test conditions and supporting optimum materials selection in the future for these components.

It appears that manufacturers choose to use certain polymers for certain types of components only. For example, while PTFE is seen in all valves (normally open or closed), manufacturer C uses PTFE in breakaways but not in fueling nozzles. Similarly, manufacturer D uses PTFE in fueling nozzles but not in breakaways. The degradation of these polymers was assessed based on the following:

a. Differences due to polymer selections for components and related chemical and physical properties changes in hydrogen environments

b. Temperature conditions with specific emphasis on cycling at cold temperatures and related thermal shock

c. Effect of the number of cycles (1000 vs 500) and corresponding mechanical and physical stresses

d. Design-related factors such as 1. O-ring thicknesses, sizes and location within the component 2. Whether it is a hydrogen-intensive location within component or not 3. Whether surrounding metal fixturing makes seal with polymer and how it moves relative to the polymer due to CTE (Coefficient of Thermal Expansion) differences

An attempt is made to summarize the data collected from more than 500 characterization analyses of specimens from a total of 49 components with an average of three O-rings in each component, using at least three techniques per O-ring type for identification of chemical and physical changes due to hydrogen effects at -40°C and -20°C, for a maximum of 1000 cycles. To limit the scope of this report, the sections below will focus on four components, namely, normally open valves, normally closed valves, breakaways, and fueling nozzles.

4.1 Normally open and normally closed valves

Normally open and closed valves are designed to regulate gas flow by opening or closing such that pressure and flow is maintained or controlled in the system without any leaks.

Normally open and closed valves, regardless of manufacturer, only had PTFE O-rings for sealing. These valves were tested at -40°C and -20°C and components were removed at 500 and 1000 cycles at each temperature. If a component failed and caused a leak, then it was removed immediately from the manifold, regardless of the cycle count and set aside for analyses.

Table 3. Normally open valves from two different manufacturers (A, B) compared for different test conditions

Test conditions	NO-B Valve IDs	ID of O rings	NO-A Valve IDs	ID of O rings	Observations	Pass or Fail
1000 cycles, -20°C	NO033	5G1, 5G2	NO003	5B1, 5B2	Fraying of PTFE	Pass
500 cycles, -20°C	NO048	5M1, 5M2	NO011	5R		Pass
1000 cycles, -40°C	NO037	No ID	NO022	No ID	Fraying of PTFE	Pass
500 cycles, -40°C	NO029	No ID	NO009	No ID		Pass

Each component did not contain more than two O-rings each as is seen in Table 3 above. For valves tested at -40°C, even though IDs were not assigned, these O-rings were still analyzed as described below.

The chemical identity of the O-rings was established using ATR-FTIR (Figure). This figure also shows that PTFE O-rings do not change chemically after exposure to hydrogen at -20°C up to 1000 cycles.

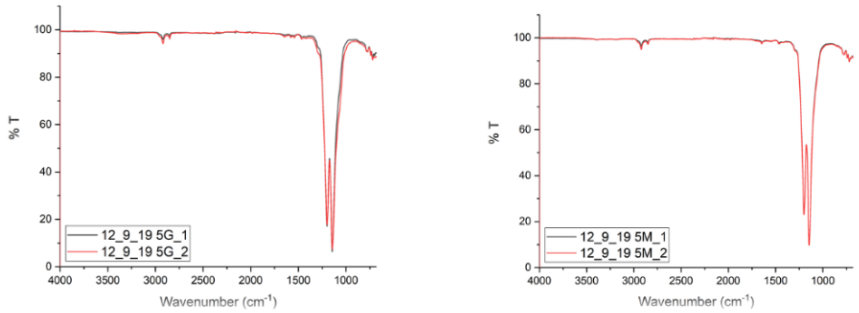

Figure 9. ATR-FTIR confirmation of chemistry of O-rings from NO-B; the black curves in both plots are for 1000 cycles, -20°C and red curves are for 500 cycles, -20°C

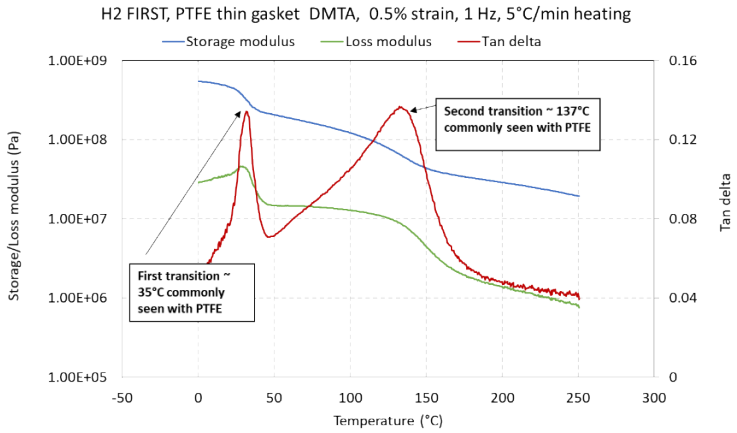

Figure 9. DMTA confirmation of chemistry of PTFE O-rings from NO-B

The glass transition temperature and storage modulus of this material, measured via DMTA, further confirmed that these O-rings were PTFE (Figure). Optical microscopy was also used to examine the O-rings. The PTFE O-rings from tested components showed massive fraying (Figure 11). In the picture, O-rings from NO-B are as frayed as the ones from NO-A but also show extensive embedded metal and other debris from the operation of the valve. This can make a difference to the hydrogen gas quality over thousands of cycles and affect other parts of the dispensing operations.

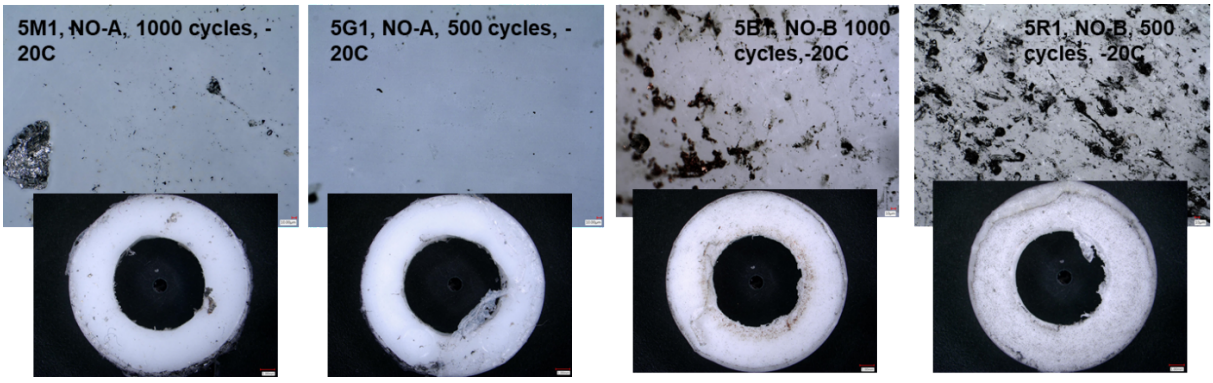

Figure 10. Keyence pictures of PTFE O-rings from NO-A and NO-B at -20°C test conditions; pictures at the top are 500X close-ups of the same O-rings

Unlike the NO valves, there were failures seen with normally close (NC) valves for low number of cycles (Table 4) at -40°C. NC047 and NC049 failed at 99 cycles.

Table 4. Normally closed valves from manufacturer NC-B tested in hydrogen at -40°C

Status	NC-B Valve IDs	Cycles	Conditions	Pass/Fail
Unexposed	NC026	0	NA	NA
Exposed	NC049	99	Minus 40C	Fail
Exposed	NC047	99	Minus 40C	Fail
Exposed	NC046	521	Minus 40C	Pass
Exposed	NC043	1017	Minus 40C	Pass

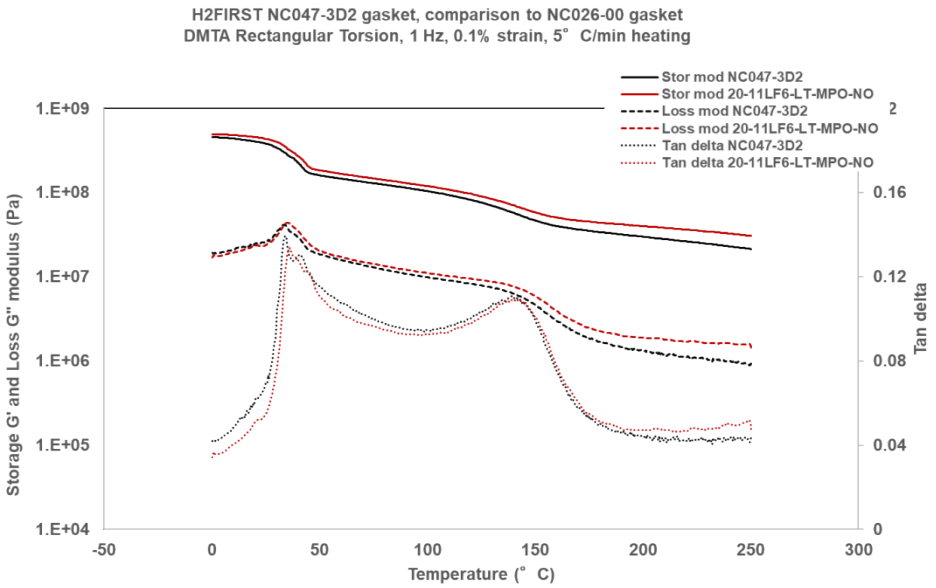

Figure 11. DMTA of normally closed valves; valve NC047 failed in testing after 99 cycles at -40°C

Investigation of O-rings from the failed valve did not show any changes in glass transition temperature nor the storage modulus which indicated that there were no chemical changes (Figure 12). Optical microscopy showed physical fraying of the O-rings from the failed component (Figure).

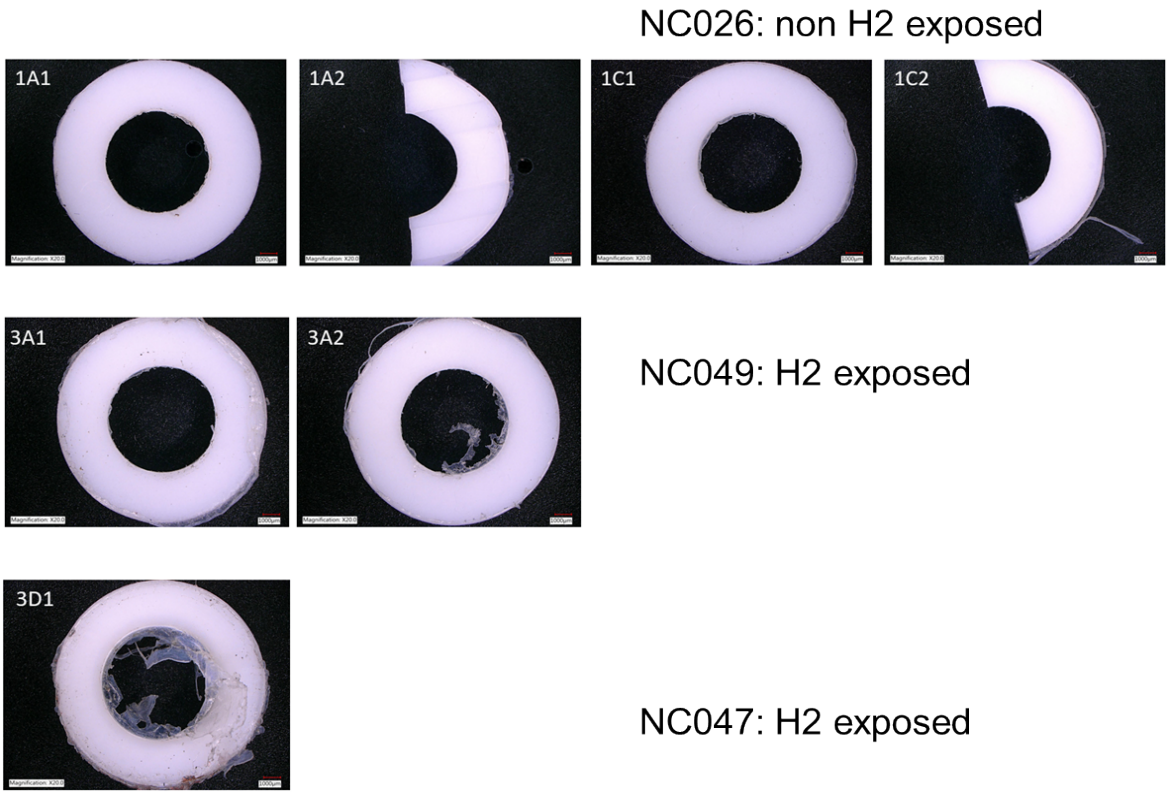

Figure 12. Keyence pictures of PTFE O-rings from unexposed NC026 and hydrogen-exposed NC047 and NC049 (all from manufacturer NO-B); NC047 and NC049 failed at 99 cycles at -40°C

However, this level of fraying was observed for PTFE O-rings in valves that passed 1000 cycles of testing and therefore, was not necessarily responsible for the failure of the NC 047 or the NC049. Another analytical technique utilized to explain the failures of the valves was nanoindentation. PTFE O-rings from the failed components were evaluated for hardness and modulus changes (Table 5).

Table 5. Nanoindentation test data on PTFE O-rings from failed normally closed valves

Normally closed valve NC-B	Hardness (GPa)	Modulus (GPa)	Hydrogen exposed?	Number of cycles @ failure, test temperature	Failure mode
NC026-B	0.064±0.02	1.58±0.35	No	NA	NA
NC049	0.068±0.01	1.53±0.19	Yes	99 cycles, -40°C	Leak at packing gland and stem interface
NC047	0.065±0.02	1.06±0.26	Yes	99 cycles, -40°C	Leaking past stem seat

Data shows that there is not much change in hardness for NC049 and for NC047. There is, however, a severe drop (~ 33%) in the storage modulus for NC047. A drop in storage modulus, proportional to stiffness, may indicate a level of plasticization of the matrix. This change in property is also supported by the extremely frayed appearance in the PTFE O-rings from NC047 compared to those from NC049 per optical microscopy examinations (Figure). It is also important to note that NREL engineers determined that the leaking at the packing gland and stem interface (where these O-rings provide a seal) was caused by insufficient torque of the seals, which were used as received from

supplier. While this is possible, if torque was initially correct for a given distance between compressing surfaces, it is also possible that when storage modulus reduced upon exposure to H2, for the same compression distance, the torque would be reduced and hence re-torqueng was necessary. When similar leaking valves were removed and re-torqued before being put back into service, they seem to continue working through the test without issues.

For PTFE O-rings in NO and NC valves, it appeared that physical damage seen as fraying in O-rings, from both passed and failed components, showed a temperature dependence. O-rings from -40°C testing (Figure : O-ring 3A2 and 3D1, 99 cycles, -40°C) showed more damage even at 99 cycles over those from components that had finished 1000 cycles at -20°C (Figure : O-ring 5B1, 1000 cycles, -20°C). However, increasing the number of cycles from 500 to 1000 cycles at -20°C (Figure) did not appear to increase the damage.

4.2 Breakaway valves

The primary function of the breakaway valves is to protect fuel-system lines from damage due to excessive separation loads, as in station drive-away incidents. These valves uncouple at a pre-determined pull-strain load and instantly seal both ends of the break, preventing costly damage to dispensers, eliminate station downtime, and avert the danger of a fuel release. Accidental disconnection can also happen with aggressive hose handling and breakaways help to quickly and safely reconnect to the pump without further damage to the dispenser.

A total of 100 breakaways from two manufacturers BR-C and BR-D (IDs are protected), 25 from each manufacturer at each temperature, were tested at NREL and of these, a total of 12 components were shipped to Sandia for materials analyses. In addition, two unexposed units from manufacturer BR-C and one unexposed unit from BR-D were supplied, and the O-rings analyzed from these control units provided materials for chemical identification of polymer type as well as baseline properties to be used to compare with O-rings to be removed from exposed components.

Unlike NO and NC valves, breakaways showed several failures at a varied number of cycles and at both testing temperatures (Table 6). Depending on polymer selection and component design, each type of breakaway responded to the accelerated tests differently. The polymers were chemically identified using the aforementioned techniques, as the design information is confidential and not available publicly.

Table 6. Breakaways received from NREL tests showing pass/fail ratios

Manufacturer	Total tested	Total received	Units Passed	Units Failed
Manufacturer BR-C	50	7 (+2 control)	4	3
Manufacturer BR-D	50	5 (+1 control)	5	0

The polymer most common to breakaways was Buna N or NBR (nitrile butadiene rubber). In addition, PTFE is present in one of the breakaways (BR-C) but absent in the other (BR-D). Table 7 shows a group of breakaways that were subjected to test temperatures of -20°C and -40°C in hydrogen environments and passed all 1000 cycles. ATR-FTIR was used to examine these O-rings for chemical changes, optical microscopy was used to look for surface changes, and DMTA was used to measure the glass transition and storage modulus changes after exposure to hydrogen.

Table 7. Breakaways from manufactures BR-C and BR-D for different test conditions

Test conditions	BR-C breakaways Components IDs	BR-D breakaways Component IDs	Pass or Fail
1000 cycles, -20°C	BR013	BR034	Pass
500 cycles, -20°C	BR016	BR056	Pass
1000 cycles, -40°C	BR021	BR031	Pass
500 cycles, -40°C	BR017	BR048	Pass

Degradation was observed, with physical blistering and increased surface roughness observed with optical microscopy, and some chemical changes observed using ATR-FTIR. In addition to the BR-C breakaways that completed 500 and 1000 cycles, four additional BR-C breakaways with passed and failed units at -40°C were also evaluated (Table 8). This group included units that had failed at 132 through 356 cycles at -40°C hydrogen. Also included was a unit that had passed 165 cycles at -40°C but, removed for comparison to the early failures. One unit that had passed 1000 cycles (similar to the BR021, BR017) was also in this group.

Table 8. Breakaways tested in hydrogen at -40°C

Status	BR-C Breakaways	Cycles completed pass/fail	Conditions	Pass/Fail	Reasons
Unexposed	BR001	0	NA	NA	
Exposed	BR018	132	-40°C	Fail	Leaked at coupling
Exposed	BR022	214	-40°C	Fail	CGs spiked at end of fill. Leak found at the outlet of breakaway
Exposed	BR023	356	-40°C	Fail	CGs spiked at end of fill. Leak found at the outlet of breakaway
Exposed	BR017	165	-40°C	Pass	Removed for comparison to earlier failures
Exposed	BR021	1021	-40°C	Pass	

DMTA was the first analytical method used to evaluate Buna N O-rings from the BR018 unit that failed at 132 cycles at -40°C in hydrogen (Figure).

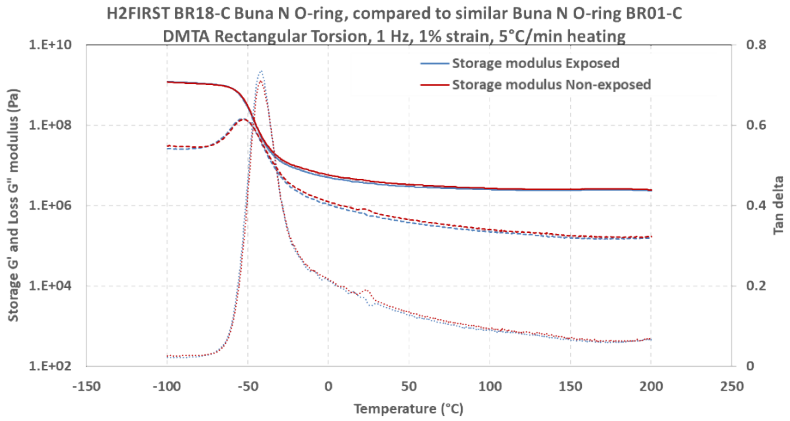

Figure 13. DMTA plot of Buna N O-ring from BR018 unit that failed at 132 cycles

As is clear from the plot, there are no dramatic changes seen in the glass transition temperature (peak of the Tan delta peak) or storage modulus values between the exposed and non-exposed O-rings. Figure shows the ATR-FTIR spectra for the same O-rings.

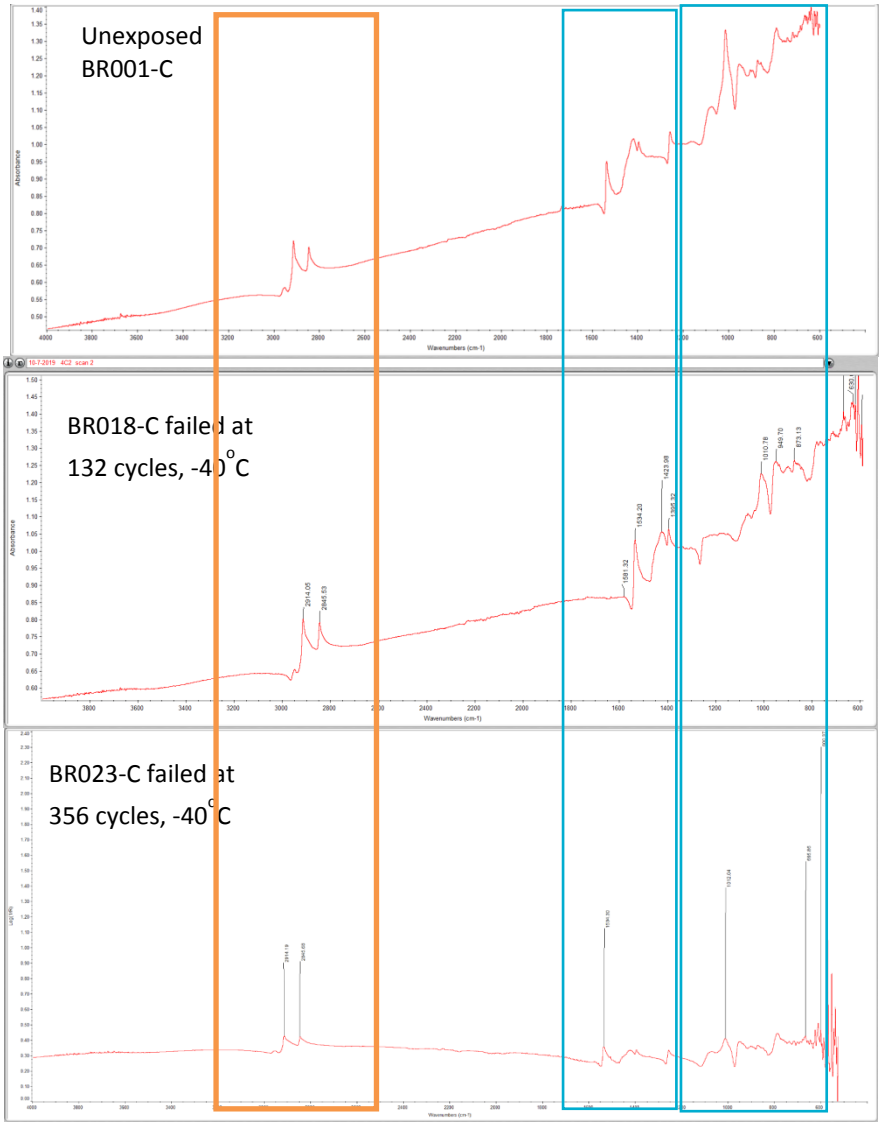

Figure 14. ATR-FTIR plots of BR-C units: unexposed to hydrogen BR-001 (top), BR018 failed at 132 cycles at -40°C (middle), BR023 failed at 356 cycles, -40°C (bottom)

ATR-FTIR did not show any specific changes in Buna N O-rings except for a decrease in peak intensity for the sample at 356 cycles. This technique is focused on chemical analysis of the surface of the sample and if there is not good contact of the ATR crystal tip with the sample, it is difficult to obtain a good spectrum. This is likely the cause of the decrease intensity for the 356-cycle sample. This is specifically a problem with soft rubbery materials such as Buna N because of its resilience. A recommended method is to microtome the sample and take 10 to 15-µm thickness of the same O-ring for ATR-FTIR. In future work with polymers, we plan to employ this technique for sharper FTIR spectra.

Optical microscopy of Buna N O-rings from BR-C breakaways revealed massive change in surface texture with minute blisters over the surface (Figure a). In addition to blistering, some of the Buna N O-rings from BR-C units that had failed at 356 cycles at -40°C showed a flattening along the axis of

the O-rings with debris present in the flattened portion (Figure b). For PTFE O-rings present in the same BR-C breakaway, there were cracks seen in the middle along with frayed edges and swelling of the O-ring (inset) (Figure c).

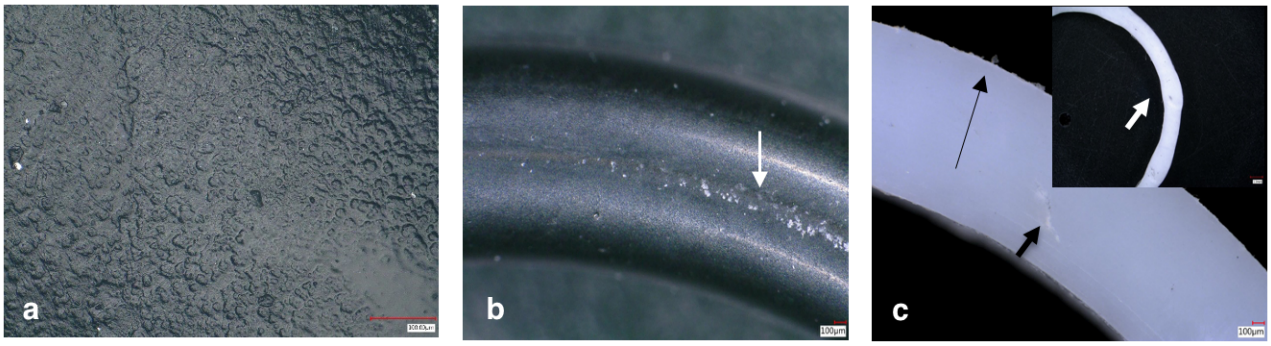

Figure 15. Optical microscopy pictures of BR-C O-rings, which (a) passed 500 cycles at -20°C and (b, c) failed at outlet after 356 cycles at -40°C: a = Blistering of Buna N; b = flattening of Buna N O-ring, debris present; c = cracking, fraying and swelling of PTFE

Just like with the PTFE O-rings in normally closed valves, nanoindentation was used to check for hardness and modulus changes with the BR018 PTFE O-rings (Table 9). A significant decrease in hardness and elastic modulus was observed indicating possible plasticization of the PTFE matrix due to hydrogen exposure at -40°C. This was the first indication of an actual component failing due to chemical degradation caused by hydrogen.

Table 9. Nanoindentation test data on PTFE O-rings from failed breakaways

Breakaway BR-C	Hardness (GPa)	Modulus (GPa)	Hydrogen exposed?	Number of cycles @ failure, test temperature	Failure modes
BR001-C PTFE	0.11 ± 0.02	1.68 ± 0.24	No	N/A	N/A
BR018-C PTFE	0.07 ± 0.02	1.26 ± 0.18	Yes	132 cycles, -40°C	Leak at outlet of breakaway coupling

From analysis of BR-C breakaway failures, it was concluded that degradation was more severe at -40°C compared to -20°C because all failures happened only at the lower temperature. Physical damage due to hydrogen was observed on both Buna N and PTFE. A chemical mechanism of attack (plasticization of matrix) was also observed with PTFE in BR-C breakaways.

The BR-D breakaways did not fail in any of the exposure tests. In order to understand the contribution of polymer choice and design aspects, we decided to evaluate the units that passed all testing. To this effect, several exposed breakaways of this type were disassembled and evaluated against O-rings from the unexposed unit of the same type. BR-D breakaways used Buna N O-rings along with other polymers such as butyl rubber, PEEK, thermoplastic and elastomeric polyurethanes (TPU). This was determined using ATR-FTIR and DMTA (plots not shown here). Unlike the Buna N in the BR-C design, BR-D Buna N O-rings are not exposed directly to hydrogen and therefore showed very little hydrogen effects. However, it was observed that the butyl rubber and the TPU in the BR-D components had measurable changes after exposure to hydrogen at -20°C and -40°C for 500 and 1000 cycle sets (Table 10 and Table 11). Butyl rubber shows a significant increase in storage modulus and the thermoplastic polyurethanes show little change in storage modulus with increasing test

temperature and number of cycles (Figure 1). Glass transition temperature increased in butyl rubber but did not change much in thermoplastic polyurethanes (referred to as proprietary PUR #2 in plots) with increasing test temperature and number of cycles (Figure 1).

Table 10. DMTA data on BR-D breakaways at -40°C

Breakaways	Polymer	Storage modulus (MPa)	Tan Delta Peak 1 (degree C)
BR031-D (1000 cycles, -40°C)	Butyl rubber	60.47±13.34	-6.77±0.44
	Proprietary PUR #2	14.87±0.49	-29.31±0.65
BR048-D (500 cycles, -40°C)	Butyl rubber	53.08±1.58	-7.53±0.07
	Proprietary PUR #2	14.30±0.66	-31.75±0.10

Table 11. DMTA data on BR-D breakaways at -20°C

Breakaways	Polymer	Storage modulus (MPa)	Tan Delta Peak 1 (°C)
BR034-D (1000 cycles, -20°C)	Butyl rubber	55.9 ± 8.4	-6.1 ± 0.50
	Proprietary PUR #2	13.4 ± 0.5	-29.5 ± 0.40
BR056-D (500 cycles, -20°C)	Butyl Rubber	47.6 ± 7.5	-8.3 ± 0.4
	Proprietary PUR # 2	13.80 ± 0.90	-29.80 ± 1.9

In spite of these distinct changes in mechanical properties, they were not significant enough to cause failure in the BR-D units even under the test conditions of the study. However, it is possible that if these BR-D breakaways were tested for 1000s of cycles in hydrogen at -40°C, polymers in these components may degrade further so as to give new and different modes of component failure.

In general, for breakaways, physical damage was observed to be the predominant cause of component failure in hydrogen service. Buna N, PTFE, PEEK, butyl rubber, elastomeric and thermoplastic polyurethanes have shown vulnerability with increasing number of cycles and lowering of test temperatures.

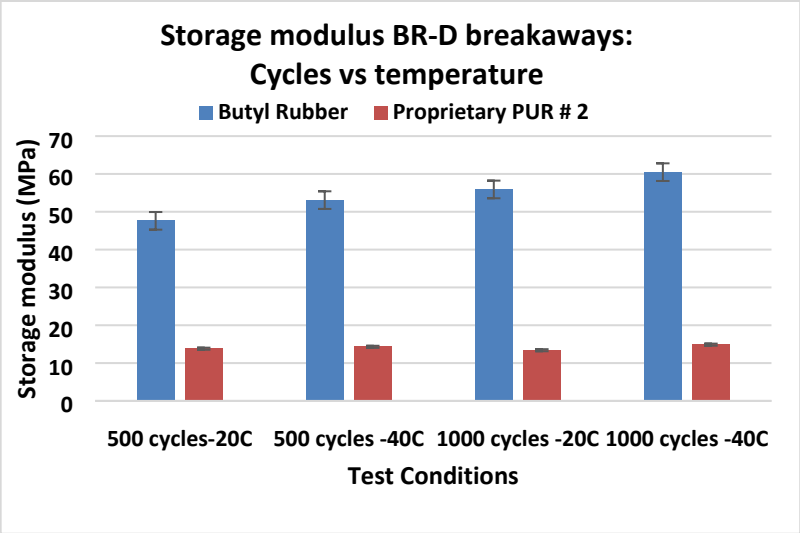

Figure 17. Storage modulus changes in Butyl rubber and polyurethane in BR-D breakaways with cycling at -20°C and -40°C

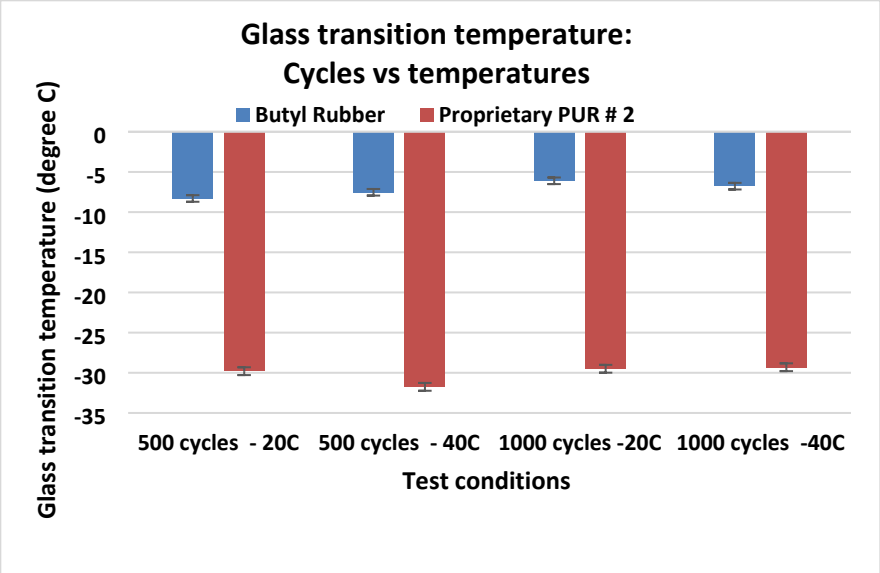

Figure 18. Glass transition temperature T_g changes in Butyl rubber and polyurethane in BR-D breakaways with cycling at -20°C and -40°C

Optical microscopy of butyl rubber, thermoplastic polyurethanes, and PEEK from BR-D breakaways showed major changes in surface texture and, in some cases, severe attack by hydrogen. Exposures at lower temperatures increased blistering and created deep grooves in the thermoplastic polyurethane and increased wear in PEEK, but temperature and cycling only marginally affected the butyl rubber, likely due to its lack of hydrogen exposure in these breakaways.

Though the glass transition temperatures of the elastomeric PUR and the butyl rubber are quite close (DMTA T_g for elastomeric PUR = -10.5C; T_g for butyl rubber = -6.8C), they are both above the test temperatures of -20°C and -40°C. The rigid, glassy state of both materials at these low temperatures will slow hydrogen diffusion through the polymer. The elastomeric PUR was more affected by hydrogen diffusion conditions compared to the butyl rubber.

The butyl rubber showed little surface effects (blistering, roughening) and increasing the number of cycles from 500 to 1000 did not increase damage externally for the BR-D butyl rubber O-rings.

Figure 16Figure 17 are optical microscopy images of polyurethane elastomers after cycling at -40°C and -20°C. Increasing the number of cycles at each test temperature increased damage for this material. Increased damage also occurred from lowering the exposure temperature from -20°C to -40°C for a constant cycle count. For example, after 1000 cycles at -20°C, there are distinct striations on the surface (Figure 17, right) and not only striations but also blisters after 1000 cycles at -40°C (Figure 16, right).

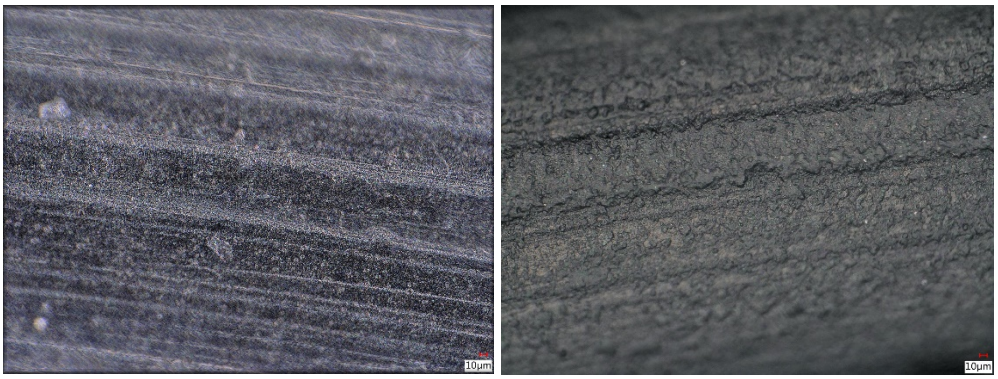

Figure 16. Optical microscopy of polyurethane elastomer from BR-D after 500 cycles (left) and 1000 cycles (right) in hydrogen at -40°C

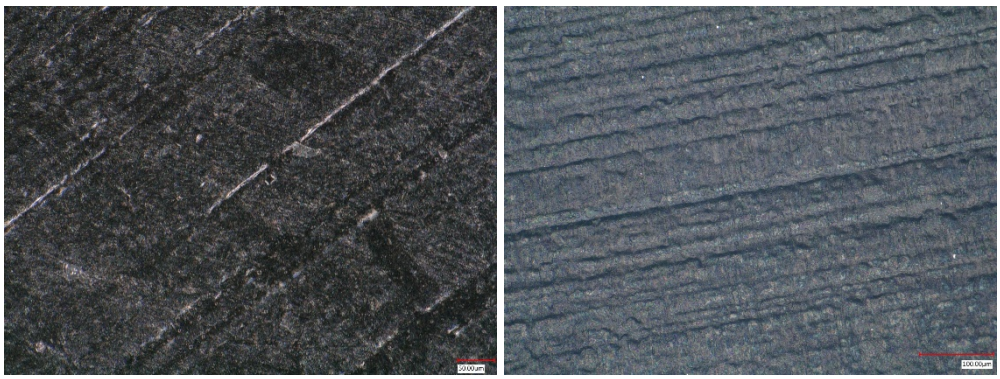

Figure 17. Optical microscopy of polyurethane elastomer from BR-D after 500 cycles (left) and 1000 cycles (right) in hydrogen at -20°C

Figure 18Figure 19 are images for butyl rubber O-rings from BR-D breakaways. For butyl rubber, increasing the number of cycles at a given temperature did not appear to increase the damage, but lowering the temperature from -20°C to -40°C for a constant number of cycles seemed to increase damage to the polymer. More striations (upper right corner of 1000 cycle -40°C of Figure 21), more pitting and gouging (center of the same picture) compared to 1000 cycles at -20° of Figure 22 is evidence for the degrading influence of hydrogen gas at the lower temperature.

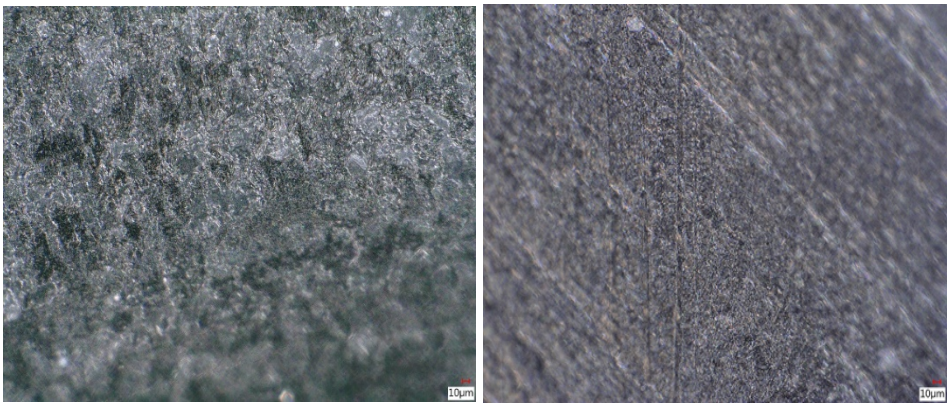

Figure 18. Optical microscopy of Butyl rubber from BR-D after 500 cycles (left) and 1000 cycles (right) in hydrogen at -40°C

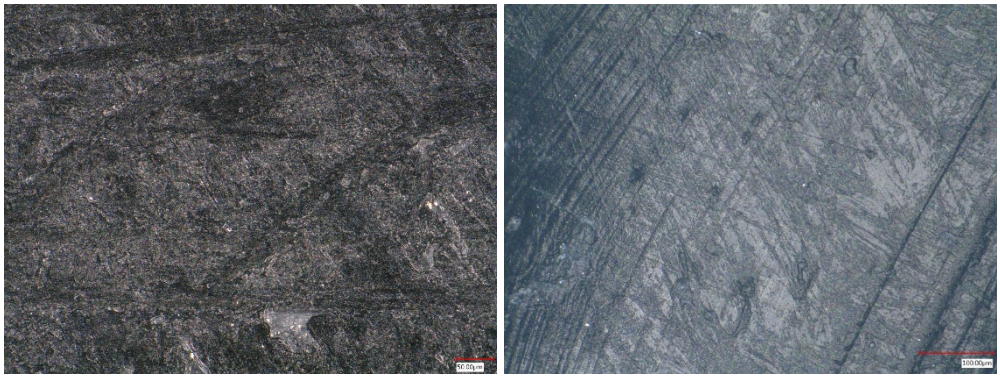

Figure 19. Optical microscopy of Butyl rubber from BR-D after 500 cycles (left) and 1000 cycles (right) in hydrogen at -20°C

Figure 20Figure 21 are images of PEEK in the BR-D breakaway after exposure to hydrogen. This material showed some damage in the form of slightly increased swelling and blistering after just 500 cycles at -20°C. The picture for PEEK after 1000 cycles, -20°C shows the blistering a little better than the 500 cycles at -20°C , though increasing the number of cycles at -20°C did not increase the extent of damage. When this material was tested in hydrogen at even lower temperatures (-40°C), extent of damage was much greater than at -20°C. The effects of cycling are also evident; at a given temperature, the blistering is much more pronounced for 1000 cycles. Severe blisters in the PEEK appear to tend to pop or form pock marks on the surface. It is clear that lowering the hydrogen temperature and increasing the number of cycles at a given temperature affected PEEK negatively.

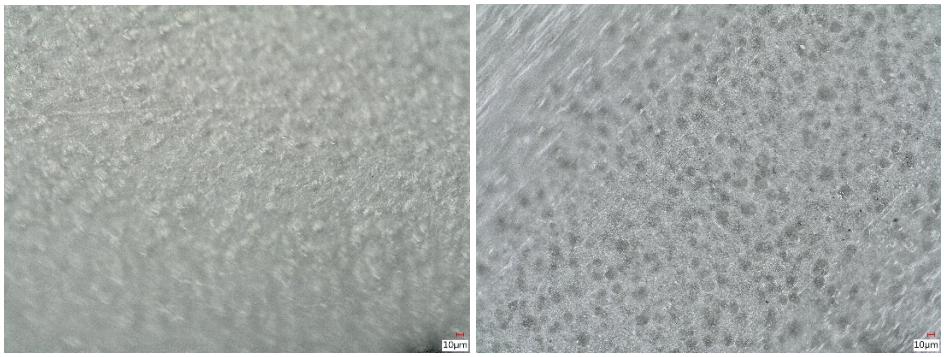

Figure 20. Optical microscopy of PEEK from BR-D after 500 cycles (left) and 1000 cycles (right) in hydrogen at -40°C

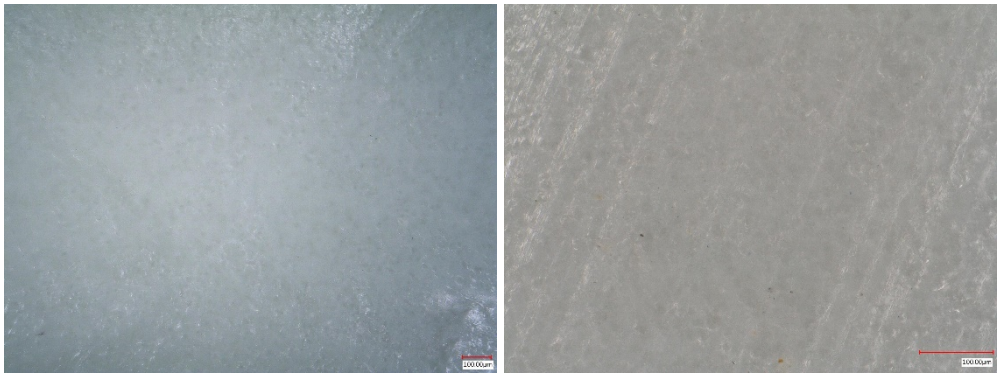

Figure 21. Optical microscopy of PEEK from BR-D after 500 cycles (left) and 1000 cycles (right) in hydrogen at -20°C

In general, for breakaways, physical damage was observed to be the predominant cause of component failure in hydrogen service. Buna N, PTFE, PEEK, butyl rubber, elastomeric and thermoplastic polyurethanes have shown vulnerability to hydrogen attack. Effects are more pronounced with increasing cycles and lower test temperatures. Depending on the design of the component, the polymers showed more or less vulnerability to hydrogen. This study has pointed out the combined importance of proper component design/engineering with careful selection of polymeric materials for longer term reliability of breakaways, a key component in dispenser system.

4.3 Fueling nozzles

Fueling nozzles are an integral part of the dispenser system. Attached to the dispenser unit and pump via hose and breakaway, the nozzle permits the transfer of pre-cooled hydrogen into the fuel tank onboard the vehicle. A total of 50 fueling nozzles each from two manufacturers FN-C and FN-D (IDs are protected) were tested at NREL and of these, a total of 10 components were shipped to Sandia for materials analyses. In addition, one unexposed nozzle from each manufacturer was supplied, and O-rings analyzed from these control units provided materials for chemical identification of polymers as well as baseline properties to be used to compare with O-rings from exposed components.

Like the breakaways, fueling nozzles showed failures at varied number of cycles and at both testing temperatures (Table 12). Depending on polymer choice and component design, each type of failure responded to the accelerated tests differently. While polymers were chemically identified using the aforementioned characterization methods, design information is confidential and not available

publicly. Differences in the designs were highlighted by the difference in the number of O-rings removed from the components.

Table 12. Fueling nozzles received from NREL tests showing pass/fail ratios

Manufacturer	Total tested	Total received	Units Passed	Units Failed
Manufacturer FN-C	50	7 (including control)	5	2
Manufacturer FN-D	50	5 (including control)	5	0

The polymer common to the two breakaways designs was PEEK (Polyether ether ketone). In addition to PEEK, Buna N, PTFE, and FKM are present in these components. Table 13 shows a group of breakaways that were subjected to test temperatures of -20°C and -40°C in hydrogen environments, all of which survived the cycling without failure.

Table 13. Fueling nozzles from manufactures FN-C and FN-D for different test conditions

Conditions (Cycles/temperature)	FN-C Fueling nozzles Components IDs	FN-D Fueling nozzles Components IDs	Pass/Fail
1000, -20°C	FN018	FN033	Pass
500, -20°C	FN004	FN040	Pass
1000, -40°C	FN022	FN026	Pass
500, -40°C	FN023	FN036	Pass

In addition to the units that passed the full number of cycles, several FN-C fueling nozzles with a different number of cycles were also evaluated (Table 14). This group included a unit that had failed at 344 cycles at -40°C in hydrogen. Also included was a unit that had passed 500 plus cycles at -40°C. Interesting contrasts included units such as FN018 which passed 1000 cycles at -20°C and FN019 which failed immediately after 1063 cycles at -20°C.

Table 14. FN-C fueling nozzles tested in hydrogen at -20°C and -40°C

Status	FN-C fueling nozzles	Cycles	Conditions	Pass/Fail	Reason for failure
Unexposed	FN001	0	NA	NA	
Exposed	FN014	344	-40°C	Fail	Leak found at the nozzle/receptacle interface
Exposed	FN023	521	-40°C	Pass	
Exposed	FN022	1017	-40°C	Pass	
Exposed	FN004	511	-20°C	Pass	
Exposed	FN018	1063	-20°C	Pass	
Exposed	FN019	1063	-20°C	Fail	Leak from the nozzle stopped the testing and no fills were done after this failure at 1063 cycles

To evaluate the effect of increasing cycles at -20°C, optical microscopy images of PEEK and Buna N from FN004 and FN018 units (both from the FN-C type of fueling nozzles) are shown in Figure 22 Figure 23. FN004 had passed 511 cycles and FN022 had passed 1063 cycles at -20°C. Both Buna N

and PEEK, from the FN-C components, show increased degradation with number of cycles. The Buna N shows increased blistering while the PEEK shows increased striations developing on the surface.

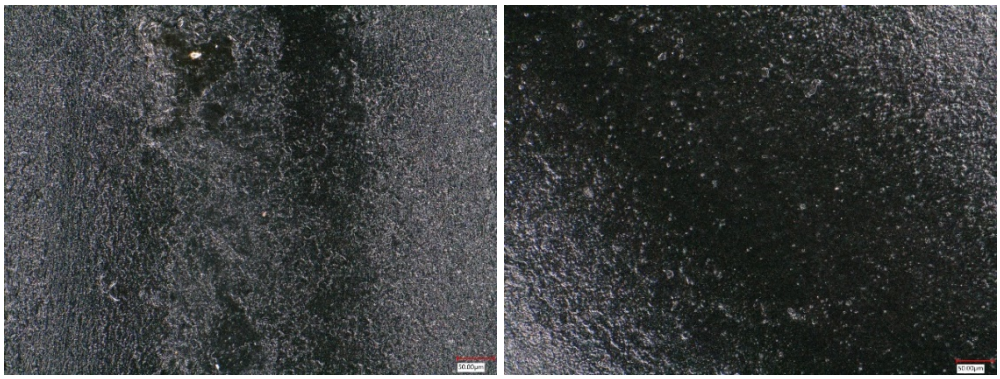

Figure 22. Optical microscopy pictures comparing Buna N from FN-C fueling nozzles (FN004 vs FN018) that were tested at 500 cycles (left) and 1000 cycles (right) at -20°C

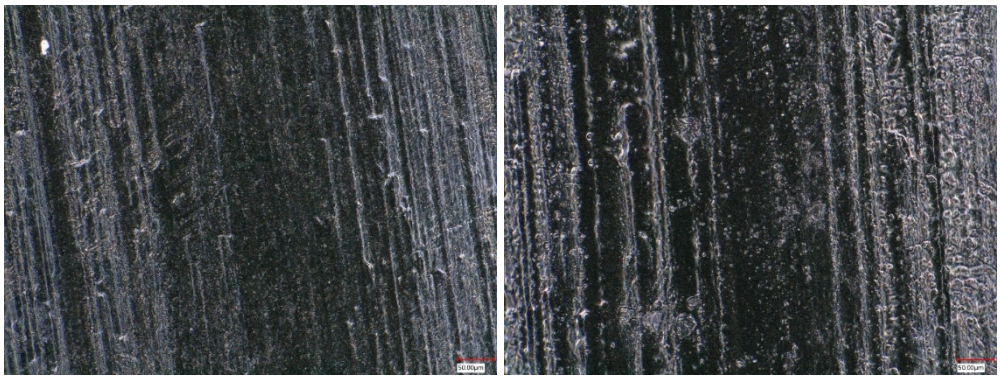

Figure 23. Optical microscopy pictures comparing PEEK from FN-C fueling nozzles (FN004 vs FN018) that were tested at 500 cycles (left) and 1000 cycles (right) at -20°C

To compare the effect of increasing cycles at -40°C, ATR-FTIR spectra of PEEK from FN023 (passed 521 cycles at -40°C) and FN022 (passed 1063 cycles at -40°C) are shown in Figure 24. The magnitude and location of several peaks shift with increased cycling at this low temperature, indicating a change in chemical composition of the surface of PEEK due to hydrogen exposure under these conditions.

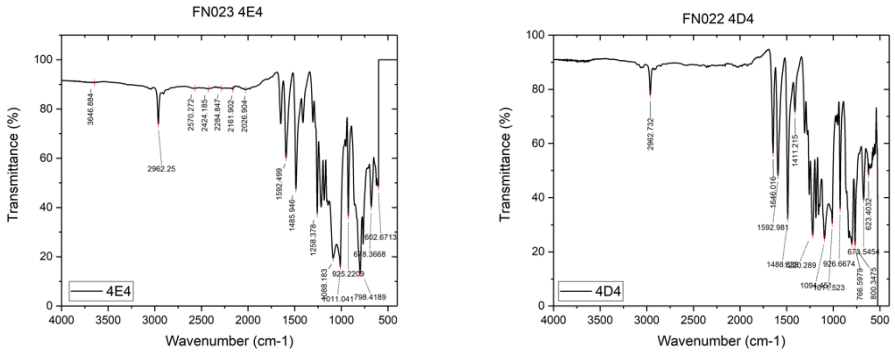

Figure 24. ATR-FTIR plots comparing PEEK from FN-C fueling nozzles (FN023 vs FN022) that were tested at 500 cycles (left) and 1000 cycles (right) at -40°C

For Buna N from -40°C testing, ATR-FTIR plots (Figure 25) and optical microscopy pictures (Figure 26) from FN023 and FN022 are shared. The FTIR plots do not show significant shifting of the peaks indicating little chemistry changes of the surface due to cycling under hydrogen at low temperature.

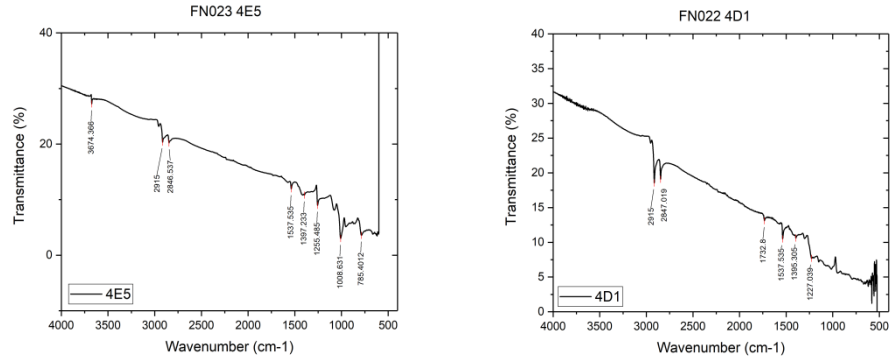

Figure 25. ATR-FTIR plots comparing Buna N from FN-C fueling nozzles (FN023 vs FN022) that were tested at 500 cycles (left) and 1000 cycles (right) at -40°C

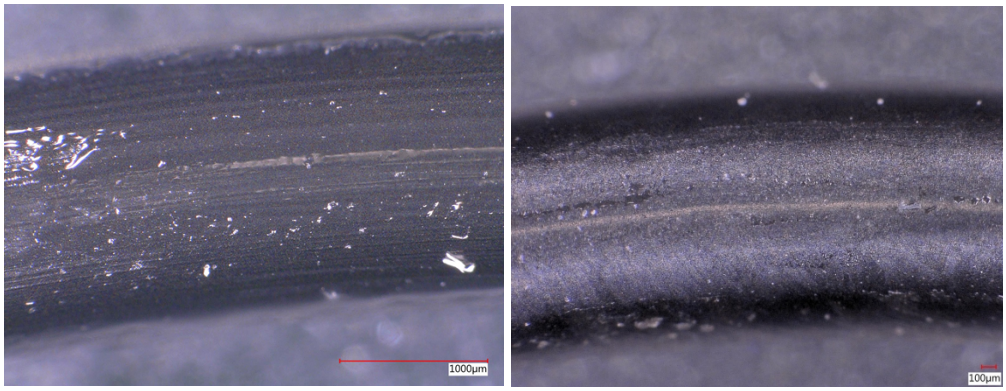

Figure 26. Optical microscopy pictures comparing Buna N from FN-C components (FN023 vs FN022) that were tested at 500 cycles (left) and 1000 cycles (right) at -40°C

Comparison of Figure 22Figure 26 and the images within Figure 26 reveals that for Buna N, the mode of degradation at decreased temperature changed from blistering to flattening with wear signs in the middle of the O-ring along the axis. This mode of failure was also seen with Buna N O-rings used in breakaways (Figure).

In order to explain the failure at 1063 cycles for FN019 fueling nozzle (Table 14), we compared the images of Buna N rubber in FN018 and FN019. FN018 had passed 1063 cycles at -20°C, whereas FN019 had failed/leaked immediately after finishing 1063 cycles at -20°C. As ATR-FTIR of Buna N in each of these components did not show any major differences, optical images of this polymer in the two components were compared (Figure 27). The degradation was found to be quite different. Where the Buna N from FN018 had blisters all over with slight flattening in center, the O-ring from FN019 showed extreme pitting and wear, possibly resulting in the failure of component FN019 after 1063 cycles. The exact reason for this difference is not well understood. If the component FN018 was cycled further, it is conceivable that it may have reached a similar point of degradation and failure.

Figure 27. Buna O-rings from FN018 (top) and FN019 (bottom) fueling nozzles that showed different extents of degradation for the same number of cycles in hydrogen at the same temperature (-20°C); FN018 was stopped at 1063 cycles and showed no failure while FN019 failed after 1063 cycles

For fueling nozzles FN-D, there were no component failures. However, a closer look some of the O-rings from this set revealed severe degradation (Figure 28). This indicates that even if a component passed the accelerated test, the state of the polymers within the component might be degraded sufficiently to cause component failure, perhaps imminently with further cycling, which points to a need of continued testing for longer cycles at the lowest temperature possible within hydrogen service.

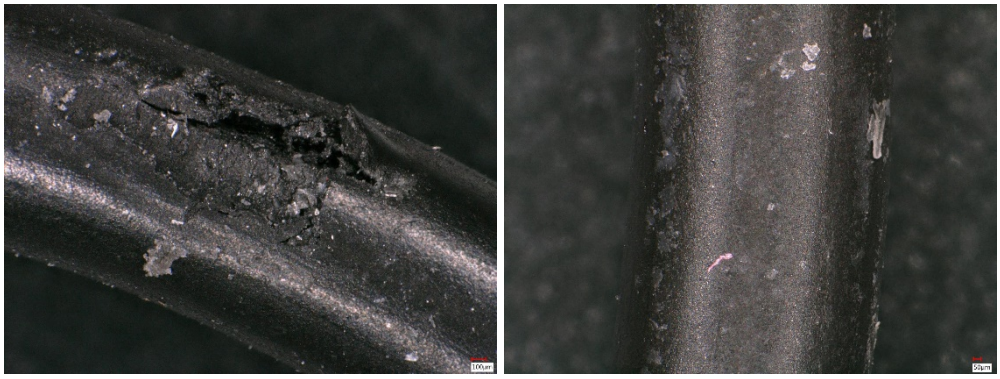

Figure 28. FN040 O-ring that passed 511 cycles at -20°C (left) and FN033 O-ring that passed 1063 cycles at -20°C (right); the shredded nature of the O-ring had not been observed with other O-rings so far

5 Conclusions

Dispensers are the top cause of maintenance events and down-time at hydrogen fueling stations. In an effort to help characterize and enable improvements in dispenser reliability, an extensive accelerated lifetime testing set-up was designed and built at NREL involving components typically used as part of dispensing operations at fueling stations. Devices Under Test (DUTs) included different components found in dispensers: normally open valves, normally closed valves, fueling nozzles, breakaways devices, and filters. The accelerated life testing included pressures and flow rates similar to light duty fuel cell electric vehicles fueling, specifically -40°C, and -20°C for over 1000 simulated vehicle fills. Tested components (failed and non-failed) were disassembled at SNL and polymeric O-rings were carefully retrieved and cataloged for chemical and physical characterization. Data was collected and comparisons were made between O-rings from unexposed (i.e., non-tested) components and those cycled in low-temperature hydrogen to characterize the hydrogen effects and failure modes. Degradation analyses, based on select polymer chemistries common across all component types, their location within components, and visual assessment of damage, coupled with strong hydrogen effects from chemical characterization, was completed.

This study fills critical knowledge gaps on the effect of pre-cooled hydrogen on dispenser components and examines deleterious hydrogen effects at these low temperatures in soft organic materials present in these components. This information can be used to improve component lifetimes, reliability, and lower dispenser maintenance costs while allowing SAE J2601 fueling protocols for a safe, fast fill at a hydrogen station. A summary of key conclusions are as follows:

1. For the 200 plus O-rings retrieved from the 71 components analyzed at SNL, the top three common polymer chemistries were Buna N/NBR (Nitrile Butadiene rubber), PTFE (Polytetrafluorethylene), and PEEK (Polyether ether ketone).

2. Overall, the failure rate amongst the components was not as high as expected for the test conditions. Among the component types tested, breakaways were the most susceptible to damage

and failed under these test conditions at a failure rate of 6%. Fueling nozzles were the next most susceptible with a 4% failure rate. Valves showed a less than 1% failure rate.

3. Two important contributing factors in a component surviving exposures at the low-test temperatures are O-ring polymer chemistry and component design. The right combination of polymer and optimum component design can make a strong difference in component reliability under severe dispenser operating conditions. Although polymer degradation may occur, it does not necessarily result in component failure. For example, in all different components which contained Buna N (NBR), many showed severe blistering and increased surface roughness with some discernable chemical changes in polymer microstructure. However, the failure rate due to Buna N O-ring degradation from low temperature hydrogen exposure was only 6% for all breakaways tested and 43% for a particular breakaway design for all the temperatures and cycles. In fueling nozzles, degradation of Buna N caused a failure rate of 4% for all units tested and 29% for one design in particular for all the temperatures and cycles. Components that showed a 100% pass with Buna N O-rings also had PEEK and PUR O-rings that showed no damage under operating conditions.

4. Physical degradation of polymers due to low temperature hydrogen exposure is more prevalent than chemical changes for these test conditions. Fraying of PTFE O-rings in NO and NC valves was severe and these O-rings often contained embedded metal fragments from adjoining metal fixtures. Buna N O-rings often exhibited severe blistering and increased roughness after hydrogen exposure. Despite the fact that some PTFE O-rings showed significant shredding and peeling at the surface (and no chemical changes) for all components, the failure rate for components with this polymer (NO valves and NC valves) was 0%.

5. As expected, increasing the number of cycles at the lowest test temperature (-40°C) increased damage. For Buna N rubber in a given component, increased cycling at -20°C did not increase the damage (blistering) as significantly as the increased cycles at -40°C. This indicates that cycling at the low temperature required by SAE J2601 of -40°C can reduce component life in fuel dispensing operations eventually leading to failure modes such as explosive decompression.

6. The nature and the extent of the degradation was much less at -20°C as compared to -40°C. The damage and failure rates were higher at lower temperatures than at higher test temperatures. The influence of exposure temperature is significant with maximum failures happening at -40°C across breakaways and fueling nozzles. The elastomers used in these components have glass transition temperatures around the test temperature (Buna N has a T_g of -40°C, polyurethane has a T_g of around -10.5°C). Above the glass transition temperature, a polymer is flexible and gas permeation through the polymer is less likely to damage the network of polymeric chains. Below the glass transition temperature, the rigid polymeric chains are more likely to break if gas diffuses into the material and forms bubbles.

6 Future work

The work under this Dispenser Reliability project will make a significant impact to addressing the lack of hydrogen refueling infrastructure and data availability. Findings from this effort, which include survival analysis and degradation analysis, will add to the qualification of dispenser components and allow for more than a pass/fail outcome.

Although 100s of components were tested in this effort under severe operating conditions (-20°C and -40°C up to a maximum of 1000 cycles) typically expected with dispenser use in hydrogen stations, the overall failure rate was lower than expected. It is clear that the influence of cycling is significant at-40°C and therefore, it is safe to assume that with more cycling, we may observe more damage

across the components. Components may exhibit failure modes that are more catastrophic, and these results can take us closer to establishing the actual lifetimes for these components for the same test conditions. A minimum of 4000-5000 cycles at -40°C would provide great evidence of polymer compatibility in hydrogen coupled with the influence of component design.

As was proven in this study, there is not much use in running these tests at temperatures higher than -40°C because maximum damage happened at the lowest test temperature.

We must consider increasing the number of components of each type for better statistical confidence in the outcomes of future tests.

We must establish the influence of component design over polymer selection if components of more varied designs are included in future work. Lower cost components may opt for completely different material choices which would warrant additional compatibility and degradation analyses.

We must also consider cycling between temperatures such as going from -40°C to +85°C (as can happen in a real fueling operation from hydrogen at -40°C to +85°C onboard a vehicle) for pressures such 750 Bar and 875 Bar.

All work must happen under collaboration and with input from component manufacturers, fueling stations, and hydrogen powered fuel cell vehicle manufacturers.

7 References

[1] “Impact of hydrogen SAE 2601 Fueling methods on fueling time of light duty fuel cell electric vehicles” Krishna Reddi. et.al. www.osti.gov 2017

[2] “Dispenser reliability Annual merit review 2019”, Peters, Mike et.al.

[3] "Investigating the Optimum Practical Hydrogen Working Pressure for Gaseous Hydrogen Fueled Vehicles," R. Harty, S. Mathison, D. Cun, M. McDougall, A. Nanalal, L. Gambone, B. J. Smith, and N. Gupta, SAE 2010 World Congress & Exhibition, SAE Technical Paper 2010-01-0854, 2010

[4] US DOE Webinar “Light Duty Fuel Cell Electric Vehicle Hydrogen Fueling Protocol” Jesse Schneider, Steve Mathison, 2017 https://www1.eere.energy.gov/hydrogenandfuelcells/pdfs/webinarslides_h2_refueling_protocols_022213.pdf